UNCLASSIFIED
SECURITY CLASSIFICATION OF THIS PAGE

REPORT DOCUMENTATION PAGE

1a. REPORT SECURITY CLASSIFICATION: UNCLASSIFIED	1b. RESTRICTIVE MARKINGS
2a. SECURITY CLASSIFICATION AUTHORITY	3. DISTRIBUTION/AVAILABILITY OF REPORT: Approved for public release; distribution unlimited.
2b. DECLASSIFICATION/DOWNGRADING SCHEDULE	
4. PERFORMING ORGANIZATION REPORT NUMBER(S)	5. MONITORING ORGANIZATION REPORT NUMBER(S): AFOSR-TR- 84-0469
6a. NAME OF PERFORMING ORGANIZATION: Drexel University	6b. OFFICE SYMBOL (If applicable)
6c. ADDRESS (City, State and ZIP Code): Department of Electrical & Computer Engineering, 32nd & Chestnut Streets, Philadelphia PA 19104	7a. NAME OF MONITORING ORGANIZATION: Air Force Office of Scientific Research
8a. NAME OF FUNDING/SPONSORING ORGANIZATION: AFOSR	8b. OFFICE SYMBOL (If applicable): NM
8c. ADDRESS (City, State and ZIP Code): Bolling AFB DC 20332	7b. ADDRESS (City, State and ZIP Code): Directorate of Mathematical & Information Sciences, Bolling AFB DC 20332
	9. PROCUREMENT INSTRUMENT IDENTIFICATION NUMBER: AFOSR-82-0110

10. SOURCE OF FUNDING NOS.

PROGRAM ELEMENT NO.	PROJECT NO.	TASK NO.	WORK UNIT NO.
61102F	2304	D9	

11. TITLE (Include Security Classification): "AN INFORMATION-THEORETIC APPROACH TO TARGET ESTIMATION OF A LASER RADAR TRACKING SYSTEM"

12. PERSONAL AUTHOR(S): Paul R. Kalata

13a. TYPE OF REPORT	13b. TIME COVERED	14. DATE OF REPORT (Yr., Mo., Day)	15. PAGE COUNT
Final	FROM 1/11/81 TO 31/10/83	20 JAN 84	45

16. SUPPLEMENTARY NOTATION

17. COSATI CODES			18. SUBJECT TERMS (Continue on reverse if necessary and identify by block number)
FIELD	GROUP	SUB. GP	

DTIC ELECTE JUN 20 1984 S D A

19. ABSTRACT (Continue on reverse if necessary and identify by block number)

High energy laser systems with highly accurate measurements as target tracking sensors use a conical scan process to obtain a target capture and tracking within the narrow beam-width. This searching process and the target tracking algorithm are major factors in the performance of the laser radar/target tracking system. Previous research results use information-theoretic concepts in establishing a laser radar/target tracking performance bound independent of the filtering algorithm. A computer program was developed to calculate the lower bound of the estimation error due to the nonlinear gaussian glint measurement process.

Applying the Extended Kalman Filter to the angle estimation problem for a gaussian glint measurement process, the resulting filter is found to have a structure consisting of a series of demodulations with gains adaptively determined by the resulting angle estimate. (CONTINUED)

20. DISTRIBUTION/AVAILABILITY OF ABSTRACT	21. ABSTRACT SECURITY CLASSIFICATION
UNCLASSIFIED/UNLIMITED ☒ SAME AS RPT. ☐ DTIC USERS ☐	UNCLASSIFIED

22a. NAME OF RESPONSIBLE INDIVIDUAL	22b. TELEPHONE NUMBER (Include Area Code)	22c. OFFICE SYMBOL
Dr. John A. Burns	(202) 767-5028	NM

DD FORM 1473, 83 APR EDITION OF 1 JAN 73 IS OBSOLETE.

SECURITY CLASSIFICATION OF THIS PAGE

AD-A142 247

DTIC FILE COPY

ITEM #19, ABSTRACT, CONTINUED: The optimal performance of this estimation process is shown to be dependent on the angle and a bound on the performance as well as a numerical algorithm is presented.

A1

An Information-Theoretic Approach
To Target Estimation of a Laser Radar Tracking System

Outline

List of Illustrations

An Information-Theoretic Approach To Target Estimation of a Laser Radar Tracking System

Dr. Paul R. Kalata
Department of Electrical and Computer Engineering
Drexel University
Philadelphia, Pennsylvania
19104

Abstract

High energy laser systems with highly accurate measurements as target tracking sensors use a conical scan process to obtain a target capture and tracking within the narrow beamwidth. This searching process and the target tracking algorithm are major factors in the performance of the laser radar/target tracking system. Previous research results use information-theoretic concepts in establishing a laser radar/target tracking performance bound independent of the filtering algorithm. A computer program was developed to calculate the lower bound of the estimation error due to the non-linear gaussian glint measurement process.

Applying the Extended Kalman Filter to the angle estimation problem for a gaussian glint measurement process, the resulting filter is found to have a structure consisting of a series of demodulations with gains adaptively determined by the resulting angle estimate. The optimal performance of this estimation process is shown to be dependent on the angle and a bound on the performance as well as a numerical algorithm is presented.

I. Introduction

A. Mathematical Model

The beam control of a highly accurate, high gain laser radar system involves an amplitude modulation/glinting/demodulation in the angle measurement process. The laser beam is controlled by a mirror to minimize the angular error between the steered (or laser pointing) angle and the target angle referenced to the laser system. The laser radar/target tracking system [1-3] is illustrated by the block diagram of Figure 1 (one dimensional). The angular measurements are developed by a glinting process created by the target and a dithered laser beam described by the following mathematical expressions.

1. Dither Signal

To generate target tracking measurements, the beam center is dithered and the returned signal is coherently correlated with that transmitted. In particular, the target/laser beam angular difference with applied dither signal is modelled by

$$y(t) = \theta_b + A \sin(\omega_d t)$$

where

θ_b is the target/beam center offset bias, and
$A \sin(\omega_d t)$ is the applied dither signal.

2. Gaussian Glint

The glint measurement process can be modeled by the deterministic gaussian function with additive noise

$$z(t) = g(y,t) + n(t)$$

where

$$g(t) = I_o \exp(-y^2/2\sigma_g^2)$$

and

$y(t)$ is the target/beam center angular error,
σ_g is a parameter of the glint return,
I_o is the reflected intensity for zero error, and
$n(t)$ is a zero mean, white noise process with variance σ_n^2.

It is to be noted that the term "gaussian" above refers to the input/output process $g(y,t)$ and is not stochastic. The additive noise term, $n(t)$, itself can be a gaussian process but it is not to be confused with the term "gaussian glint" which is the input/output functional relationship.

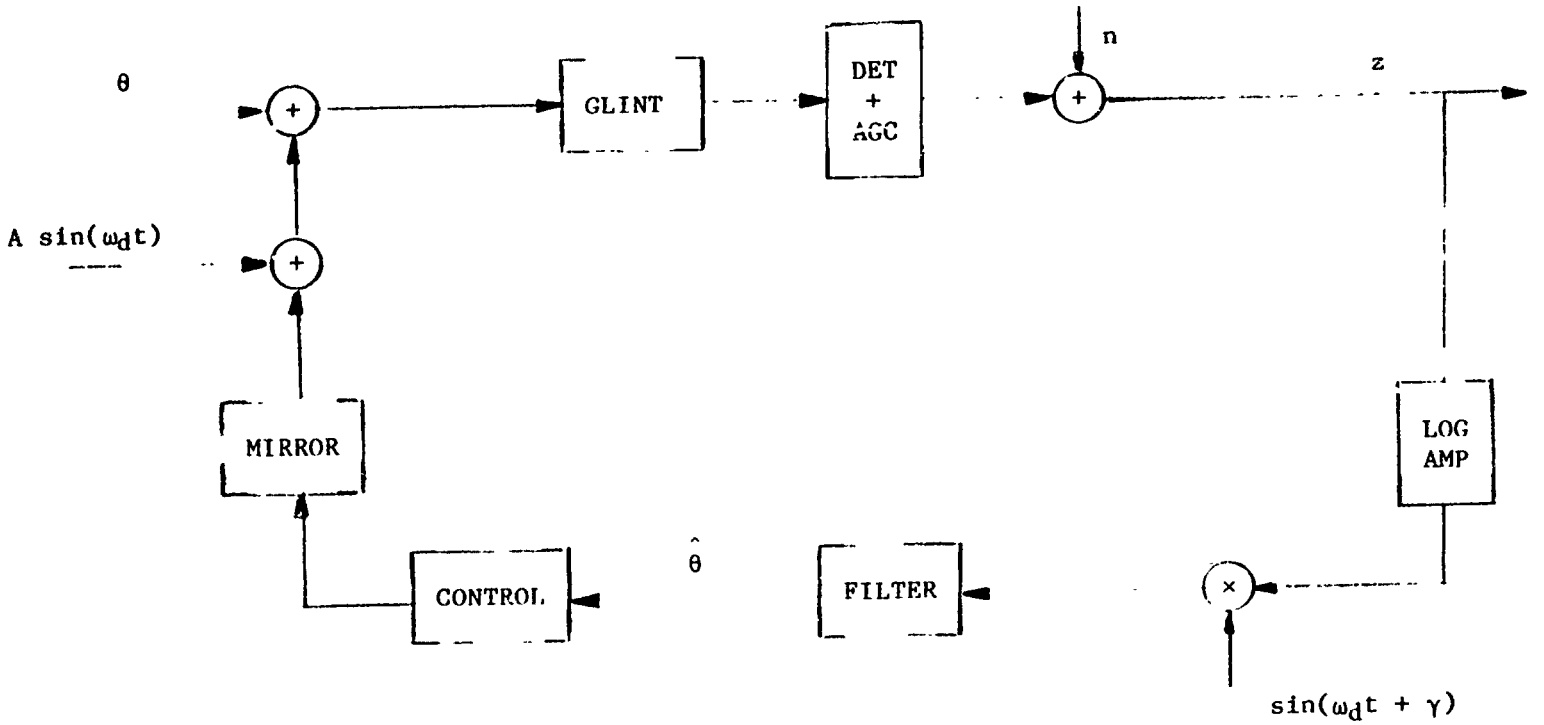

Figure 1. Laser Radar/Target Tracking Stochastic Control System

3. Signal Demodulation

The output of the gaussian glint process contains the information as to the magnitude and direction of the target/beam bias. One component of the output measurements, z(t), contains this angle bias, θ_b, as the coefficient of the base dithered signal. Hence, to recover the bias, a simple demodulation process, commonly used in Communication Systems [4], illustrated by Figure 2, includes multiplying the output by the dither signal and passing the product through a low pass filter.

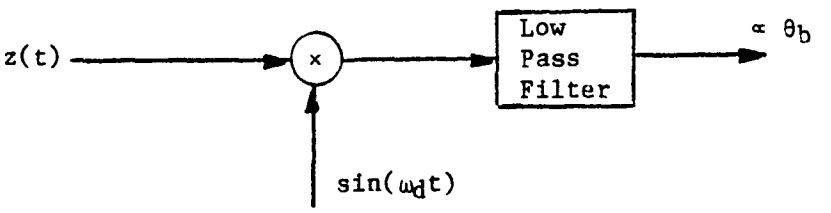

Figure 2. Glint Bias Demodulation Process

B. Statement of the Problem

The laser radar target tracking system is a stochastic control system whose objective is to track a target using noisy measurements. The performance criterion or measure of goodness of the system is given by both the closeness of the laser steered beam to the target being tracked (deterministic measure) and the variation or jitter of the steered beam (stochastic measure). In many stochastic control systems, the optimal design, choice of parameters, or operating point is usually a compromise between a set of conditions which yields the best deterministic response with that which yields the best stochastic estimates. Although the central problem addressed by this investigation is that of the stochastic design, the deterministic nature of the control system must be understood and considered. To this extent, the original [3] and current investigation centers on the problem:

> Given a laser/target tracking system with a dithered signal/gaussian glint measurement process, evaluate the Information-Theoretic estimation performance bound of the system.

The primary use of an estimation performance bound is in comparison with:

1. the performance of what is being observed with an existing filter/control system.
2. the performance of an implementable, mean-squared-error (MSE) optimal stochastic control which includes an Extended Kalman Filter.

C. Proposed and Redirected Investigation

Reference [5] contains the initial proposed research investigation of the estimation problem of the laser radar tracking system. Section II of this report contains the investigation results of tasks 1, 3, and 5. During a meeting [6] at the Air Force Weapons Laboratory, preliminary results were discussed and the investigation was redirected into the noise transfers both in the Glinting and Demodulation processes. Section III of this report contains the results of this redirected investigation.

There are two key questions on which this research investigation is centered:

1. What is the ultimate performance of the laser tracking system ?
2. What is the performance of the present process (is it sufficient, can it be made better) ?

These two areas were further investigated by considering the extended Kalman Filter described in the initial research investigation [3] and decomposing it into a Fourier Series representation. These results (Section IV) illustrate several fundamental concepts regarding the present filtering process and the performance achievable compared to the ultimate obtained through the Information-Theoretic approach.

II. Information-Theoretic Approach

A. Bounded Estimation Performance

The initial investigation [5] developed an Information-Theoretic performance bound and corresponding numerical algorithm used to evaluate an estimation performance bound for the gaussian glint measurement process which will now be summarized.

The estimation error entropy $H(\tilde{x})$ of any process is bounded by the system equivocation $H(x|z)$ with conditional probability density function $p(x|z)$, i.e.,

$$H(\tilde{x}) \geq H(x|z) \stackrel{\Delta}{=} E(-\ln (p(x|z)))$$

which is only a function of the system and independent of the implemented estimation process [7-11].

An important design concept is that the mean-square-error (MSE) estimate is a minimax error entropy estimate [10,11], i.e.,

$$\min \max H(\tilde{x}) \Leftrightarrow \min ||V(\tilde{x})||$$

where $V(x)$ is the error covariance matrix.

For the normal estimation problem [11], the derived optimal error entropy estimation process is the Kalman Filter and the error covariance matrix is identical to the system conditional covariance matrix, i.e.,

$$V(\tilde{x}) = V(x|z).$$

This is very important for understanding the Information-Theoretic approach based on prior understanding of minimal variance/Kalman Filtering concepts.

For the gaussian glint measurement process with the dither signal on the steered laser beam, the lower bound [3, 12, 13] to the error in angle estimation is

$$\sigma_{\hat{\theta}}^2 \geq \frac{1}{2\pi e} \exp(2H(\theta))\exp(2N_1(t))/\exp(2N_2(t))$$

where $H(\theta)$ is the initial angle uncertainty,

$$N_1(t) = \frac{I_o^2}{\sigma_n^2} \frac{\sigma_b}{2\sigma_\theta} \int_0^t \exp(-(\theta_b + A\sin(\omega\tau))^2/(2\sigma_b^2+\sigma_g^2))d\tau,$$

$$\sigma_b^2 = \sigma_\theta^2 \sigma_g^2/(2\sigma_\theta^2 + \sigma_g^2),$$

$$N_2(t) = \sum_{r=0,2\ldots}^{\infty} \sum_{n=r}^{\infty} \frac{t^{k-1}}{(r/2)!(n-r)!2^k} \int_0^t E(g^2(\tau)/\sigma_n^2)^k d\tau,$$

and the above integrand can be expressed

$$\int_0^t \{\cdot\} = [\frac{I_o^2}{\sigma_n^2} \frac{\sigma_c}{\sigma_\theta}]^k \int_0^t \exp(-(\theta_b + A\sin(\omega\tau))^2/(2\sigma_c^2+\sigma_g^2))d\tau$$

where $\sigma_c = \sigma_g/\sqrt{k}$.

For the initial example, a stationary target with parameters:

A = 5 normalized units
ω: f = 300 Hz
σ_g = 10
σ_θ = 10
I_o/σ_n : variable
θ_b : variable

For a signal-to-noise ratio of unity, Figures 3a to 3d are the resulting error variance lower bound for $\theta_b = \{0, 2.5, 5.0, 10\}$. Doubling the signal-to-noise results in a faster responding lower bound as illustrated by Figure 4a to 4d, $\theta_b = \{0, 2.5, 5.0, 10\}$. Notice that as the bias θ_b becomes much larger than the glint σ_g, the performance deteriorates.

B. Parametric Studies

The following lower bound performance response evaluations were made to study the effects of varying the system parameters. Figure 5 illustrates the performance response as the signal-to-noise ratio varies S/N = {1.0, 100 and 10,000} which considered a unity dither amplitude and null bias angle. It is obvious that increasing the signal-to-noise ratio improves the performance bound response.

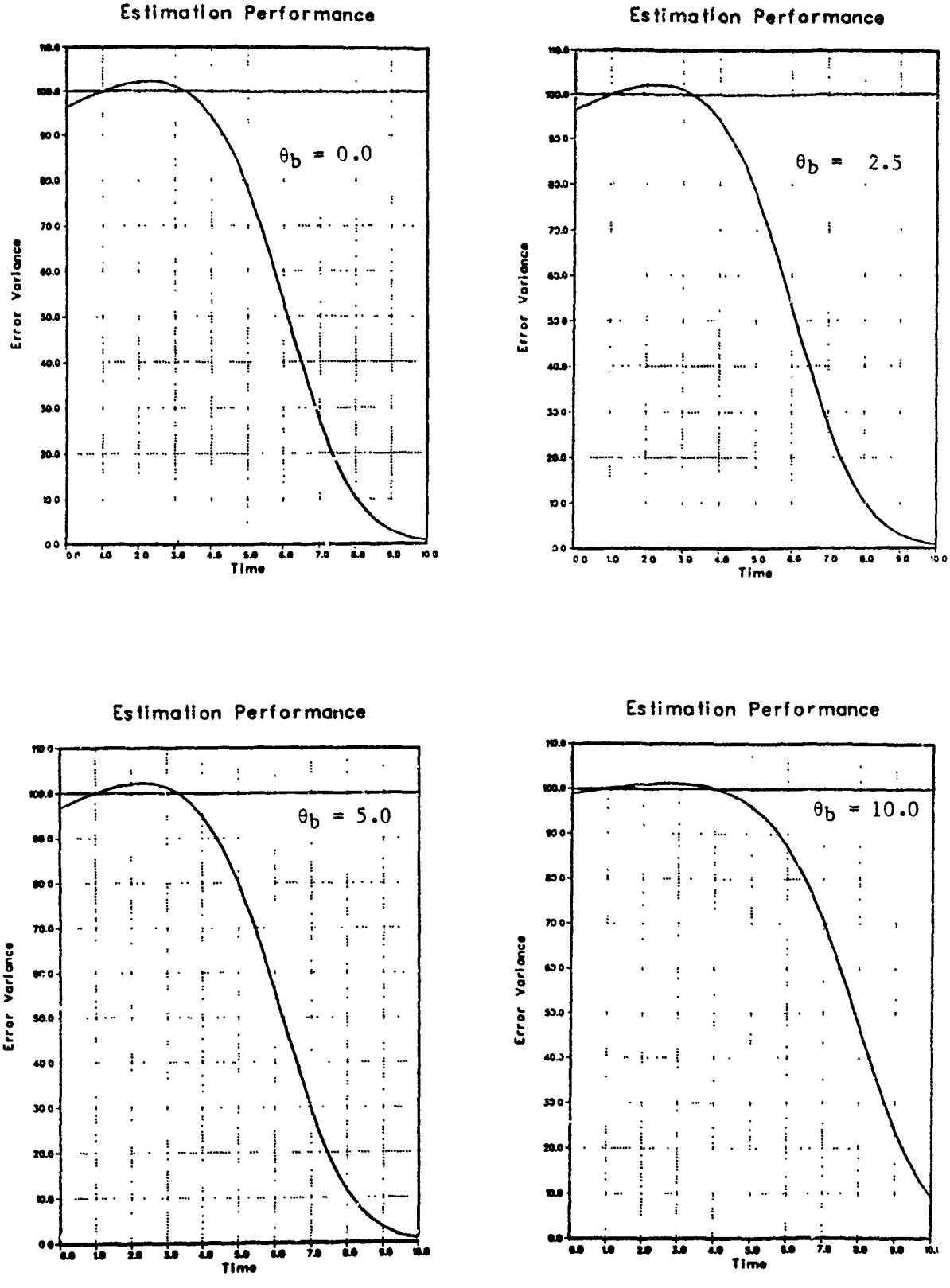

Figure 3. Error Entropy Estimation Performance Bound, S/N = 1

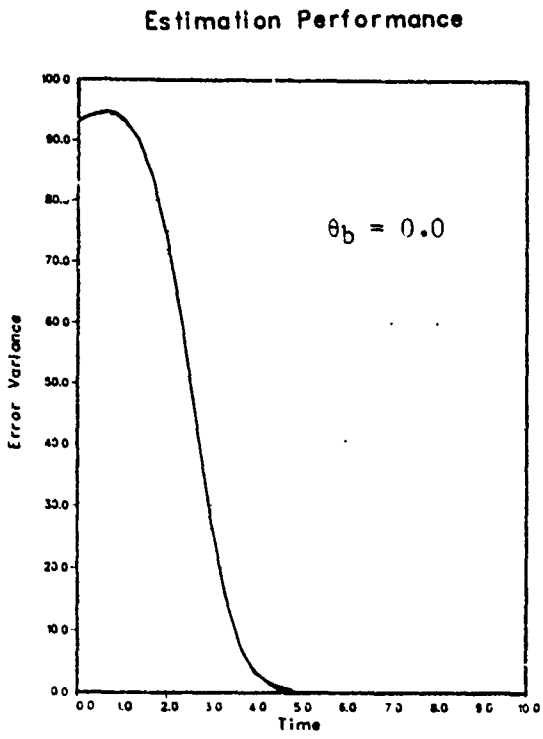

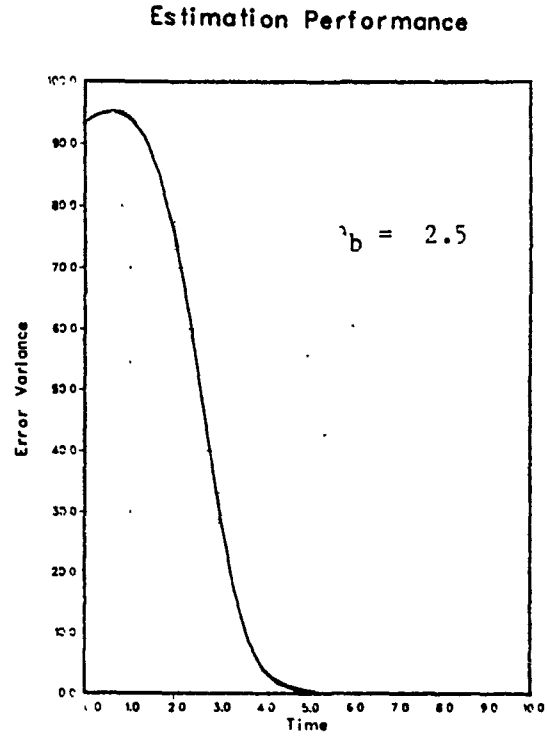

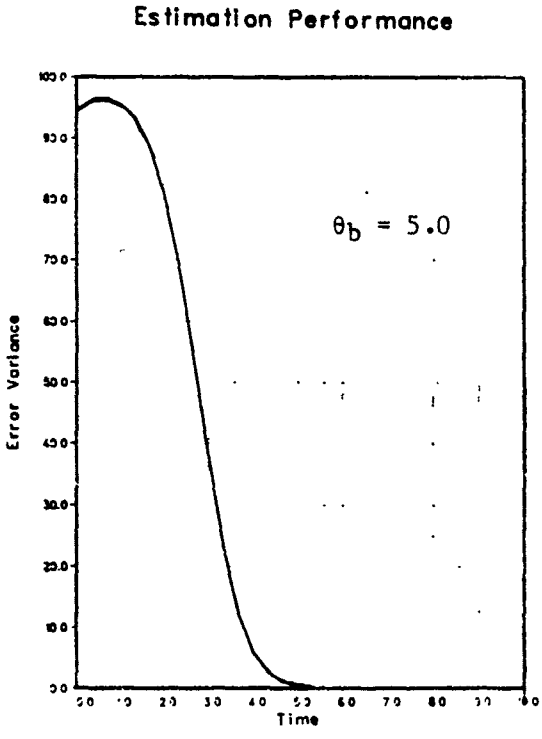

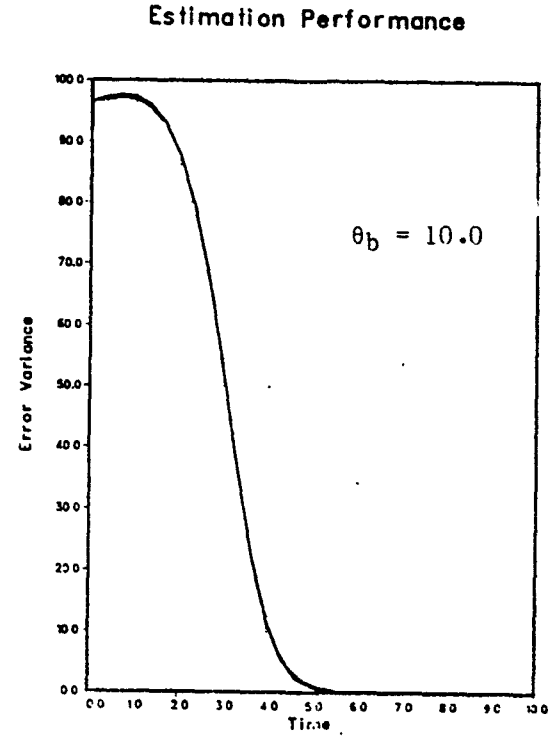

Figure 4. Error Entropy Estimation Performance Bound, S/N = 2

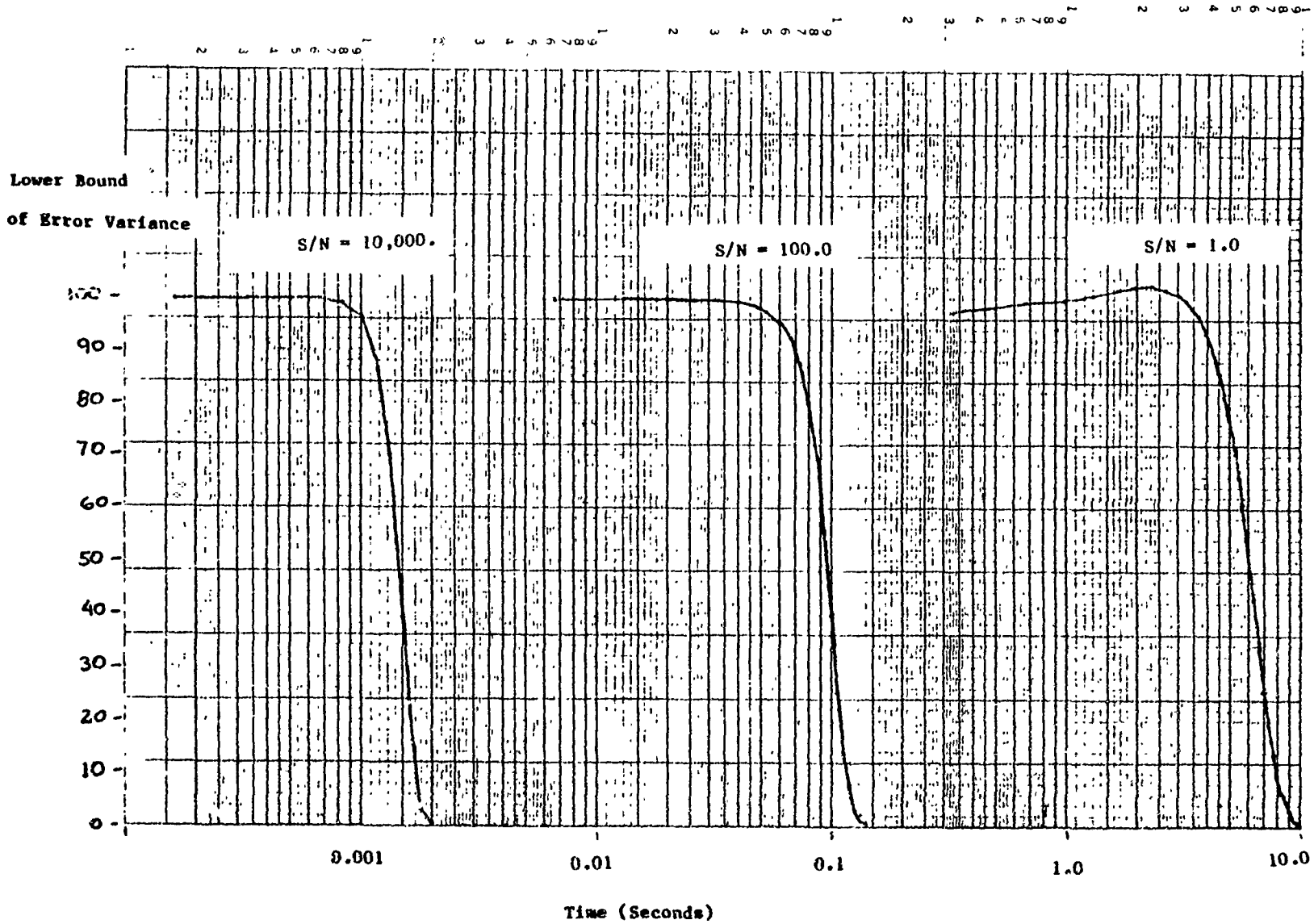

Figure 5. Error Entropy Estimation Performance Bound for Signal-to-Noise Variations

Figure 6 illustrates the case when the dither amplitude varies A = {1.0, 5.0, and 10.0} with a null bias angle and a signal-to-noise ratio of 100. The results illustrated by the figure shows that by increasing the amplitude, the performance response is slightly slower, i.e. approximately .005 seconds slower for an increase of 10 times in dither amplitude.

Figure 7 illustrates the performance found response as the bias angle change θ_b = {0.0, 5.0, 10.0} for signal-to-noise ratio of 100 and the dither amplitude unity. This illustration shows that as the angle bias varies from zero to 10, the performance bound response is approximately 10% slower.

In summary, the above parametric studies show that the "best" (fastest performance bound) response occurs as:

i) signal-to-noise increase
ii) bias angle is zero
iii) small dither amplitude

C. Information Flow Due To Demodulation

For the Laser Tracking Control system, the demodulation process illustrated by Figure 2 consists of:

1. multiplying the measurements z(t) by the fundamental frequency $\sin(\omega_d t)$, and
2. passing the results through a low pass filter to obtain an estimate of the tracking bias.

It is desired to determine if information is lost during this demodulation process. The measure of information between the unknown bias θ and the measurement z is given by

$$I(z;\theta) = H(z) - H(z|\theta)$$

where

$$z(t) = I_o \exp(-y^2/2\sigma_g^2) + n(t)$$

$$y(t) = \theta + A \sin(\omega_d t).$$

Consider a new measurement

$$z_1(t) = z(t) \sin(\omega_d t),$$

which is the first step in the demodulation estimation process. The measure of information between z_1 and θ is given by

$$I(z_1;\theta) = H(z_1) - H(z_1|\theta).$$

Using eq. (T2.4) of reference [7 or 11], the entropy of $z_1(t)$ is

$$H(z_1) = H(z) + E\{\ln|\partial z_1/\partial z|\}$$

$$H(z_1) = H(z) + E\{\ln|\sin(\omega_d t)|\}.$$

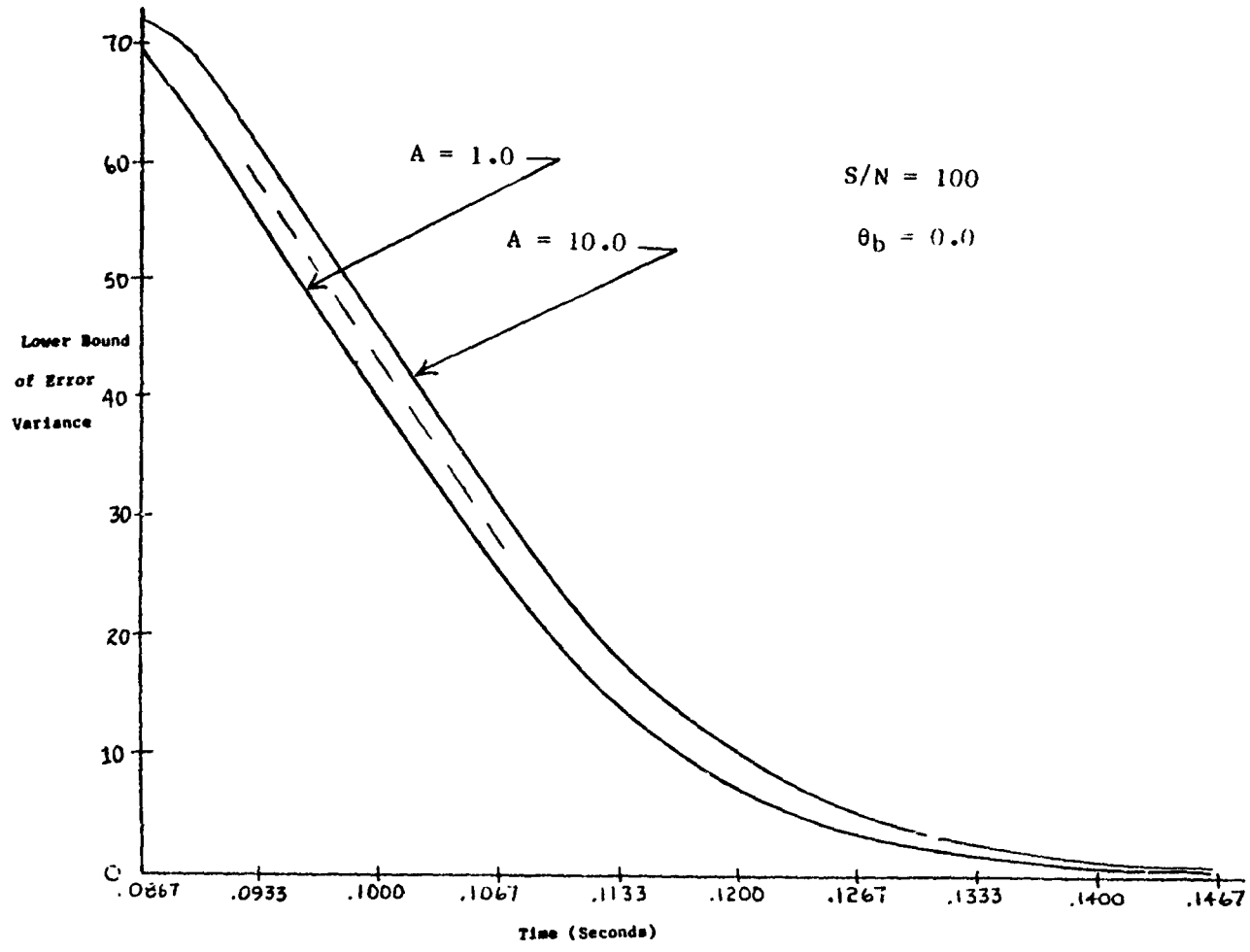

Figure 6. Error Entropy Estimation Performance Bound for Amplitude Variations

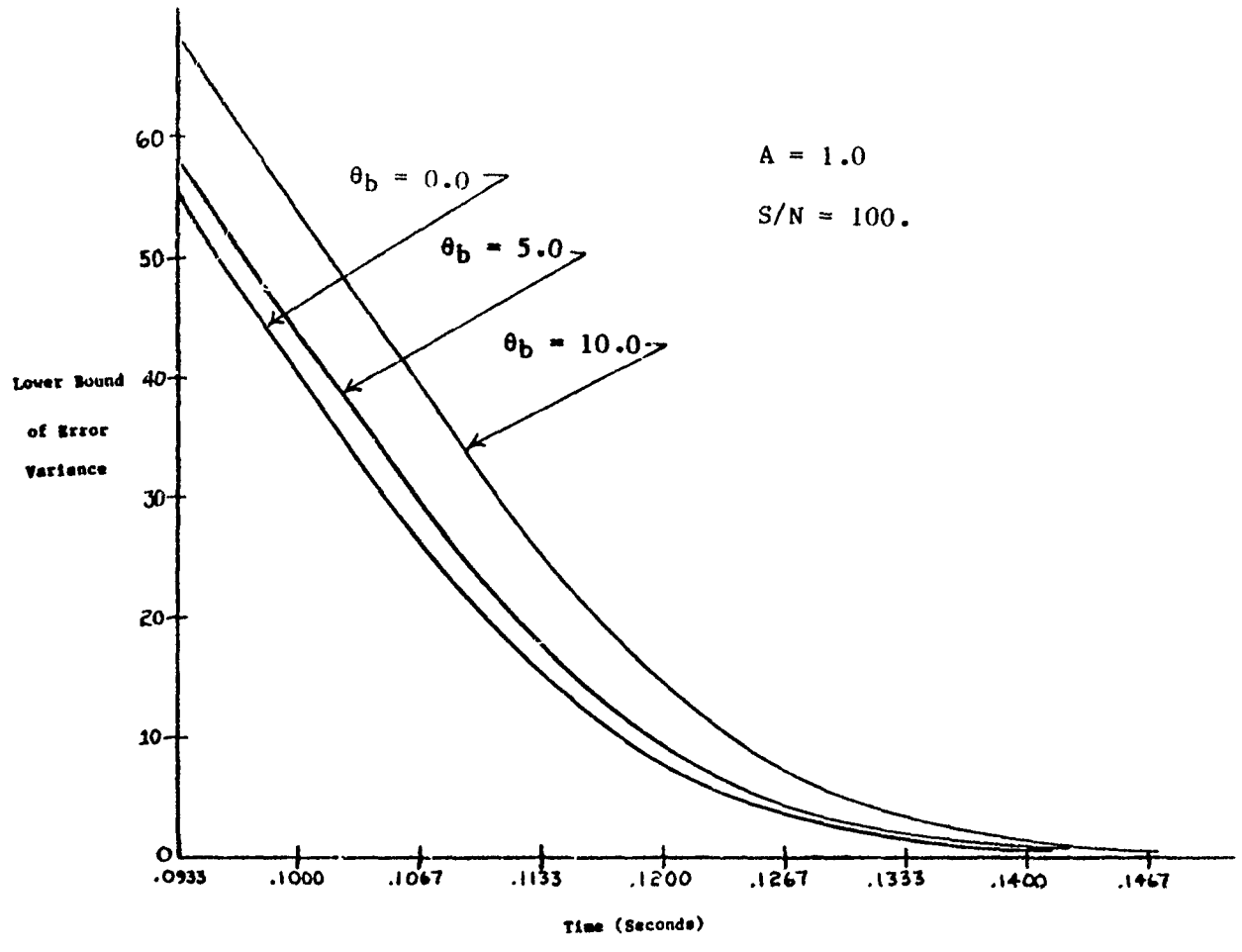

Figure 7. Error Entropy Estimation Performance Bound for Glint Bias Variations

For the conditional uncertainty term,

$$H(z_1|\theta) = H(z,\theta) + E\{\ln|\sin(\omega_d t)||\theta\}.$$

Since the process $\sin(\omega_d t)$ is independent of the unknown θ, then

$$H(z_1|\theta) = H(z|\theta) + E\{\ln|\sin(\omega_d t)|\}.$$

Combining the above two main results, it is obvious that

$$I(z_1;\theta) = I(z;\theta)$$

and no information is lost by the first step of the demodulation process.

However, the second step which involves low pass filtering, removes the information contained in the high frequency components. This point will be further explained when the extended Kalman Filter is decomposed into its Fourier Series components in Section IV. By eliminating the higher frequencies in the measurement process, information about the target is lost.

III. Glint/Filter/Control System

A. Deterministic Stability

The process of generating target angle measurements and estimates involves a dither signal/glint/demodulation process is similar to the amplitude modulation communication technique [4] as shown earlier by Figure 1. Depending on the operating or glint bias point, the received signal contains the information on the direction and magnitude of the angle pointing bias. The nature of the filter/control/mirror deterministic portion of the feedback system can be analyzed using classical techniques. The modulation/glint/demodulation process can be linearized using the first order approximations of the glint output with respect to the angle bias (neglecting the dither signal carrier) as shown in Figure 8

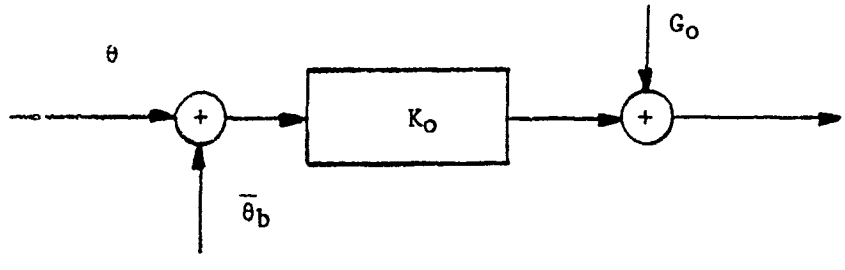

Figure 8. Linearization Model of the Gaussian Glint Process

where

Effective Gain: $K_o = - G_o \bar{\theta}_b/\sigma_g^2$

DC Level: $G_o = I_o \exp(-\bar{\theta}_b^2/2\sigma_g^2)$

Average Bias: $\bar{\theta}_b$
(operating point)

Another method to determine the effective system gain of the glinting process is to use the Fundamental Describing Function [14]. In either case, it is obviously a function of the bias operating point. The standard modulation technique consists of using a sinusoidal signal to carry the information, and in our case, it contains bias error. The bias error can be obtained by a coherent detection process which consists of multiplying the glint output (measurement) by the same sinusoidal signal and sending the resultant signal through a low pass filter. This process is essentially the mathematical process used to determine the basic Fourier Series harmonic in a periodic signal. This concept will be used in Section IV when the Extended Kalman Filter is decomposed into its basic components. The overall effective system gain will be maximum when the signal is at the gaussian glint point σ_g and vanished at zero, hence, the system gain varies according to the bias point.

Table 1 lists the various transfer functions [6,15] of the feedback path. The transfer function $H(j\omega)$ of Figure 9 illustrates the general nature of the filter/control/mirror path

$$G_f(s) = F(s)\ C(s)\ M(s)$$

$$F(s) = G_2(s)\ G_4(s) \text{ (without the notch filter } G_3(s))$$

$$C(s) = 1/s \text{ (without compensator)}$$

The effect of the notch filter $G_3(s)$ adds zeros at the dither and twice the dither frequency (300 and 600 Hz) and is intended to remove frequency modes which are caused by non-linearities and/or a non-perfect demodulation process. However, by observing Figure 9, the feedback system G(s) is basically a Type II low pass filter with an essential triple break at 150 Hz. The suppression effect of this filter on a signal at the dither frequency is large enough so that, for analysis purposes, the notch filter $G_3(s)$ will not be included. For example, there is an approximate 30 dB transfer function decreased froma frequency increase of 150 to 300 Hz which represents a 1/25 relative signal change.

The effect of the compensator $G_c(s)$ essentially stabilizes the system. Figures 10a and 10b show that Bode Plots (amplitude and phase) of the feedback system with and without the compensator which is used to provide positive gain and phase margins (gain margin of 75 dB at 35 Hz).

3. Stochastic Analysis

The demodulation process consists of multiplying the measurements with the initial dithered signal and passing the product through a low-pass system which consists of a Filter/Control subsystem. In particular, consider the process of the demodulation process as shown in Figure 2 where the noisy measurements is multiplied by $\sin(\omega_d t)$ and then passed through a low pass filter to regain the D.C. level which contains the glint bias. The noise analysis of this demodulation process considers the input noise $n_i(t)$ applied to the demodulation process is characterized by its spectral density of Figure 11.

Table 1. Transfer Functions of the Laser Radar Feedback System

Function	Transfer Functions
Band Pass	$G_2(s) = \dfrac{1}{(s/\omega_5) + 1}$; $f_5 = 150$ Hz
Notch	$G_3(s) = \dfrac{[(s/\omega_6)^2 + 1][(s/\omega_7)^2 + 1]}{[(s/\omega_6)^2 + 0.8(s/\omega_6) + 1][(s/\omega_7)^2 + 0.8(s/\omega_7) + 1]}$; $f_6 = 300$ Hz, $f_7 = 600$ Hz
Low Pass	$G_4(s) = \dfrac{2}{(s/\omega_8)^2 + 0.8(s/\omega_8) + 1}$; $f_8 = 150$ Hz
Compensator	$G_5(s) = \dfrac{0.8(s/\omega_9 + 1)}{s(s/\omega_{10} + 1)}$; $f_9 = 4$ Hz, $f_{10} = 25$ Hz
Control	$G_c(s) = 1/s$
Mirror	$M(s) = \dfrac{1}{s(s/\omega_m + 1)}$; $f_m = 350$ Hz

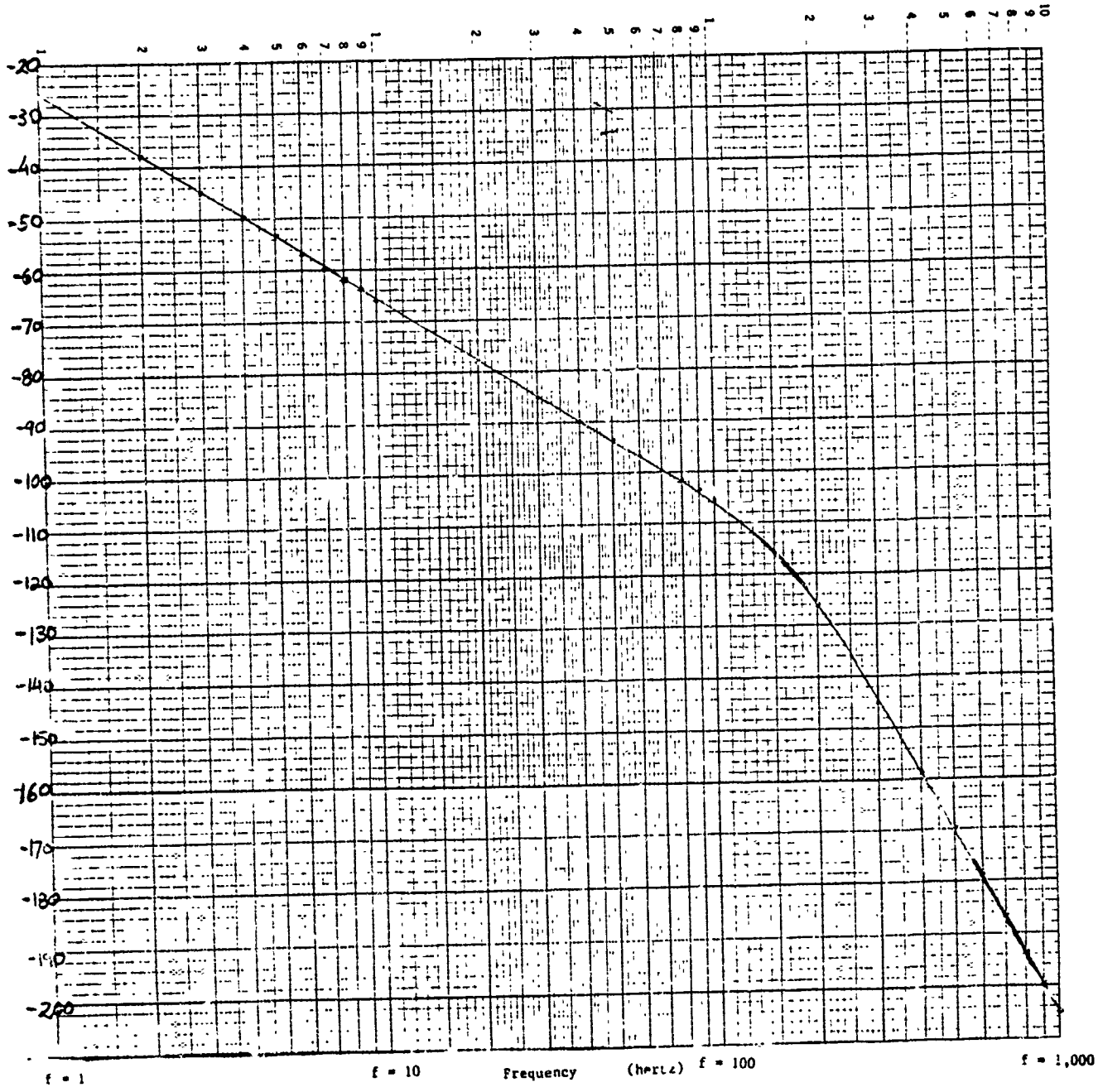

Figure 9. Frequency Response (Log Magnitude) of the Laser Filter/Control/ Mirror Feedback System

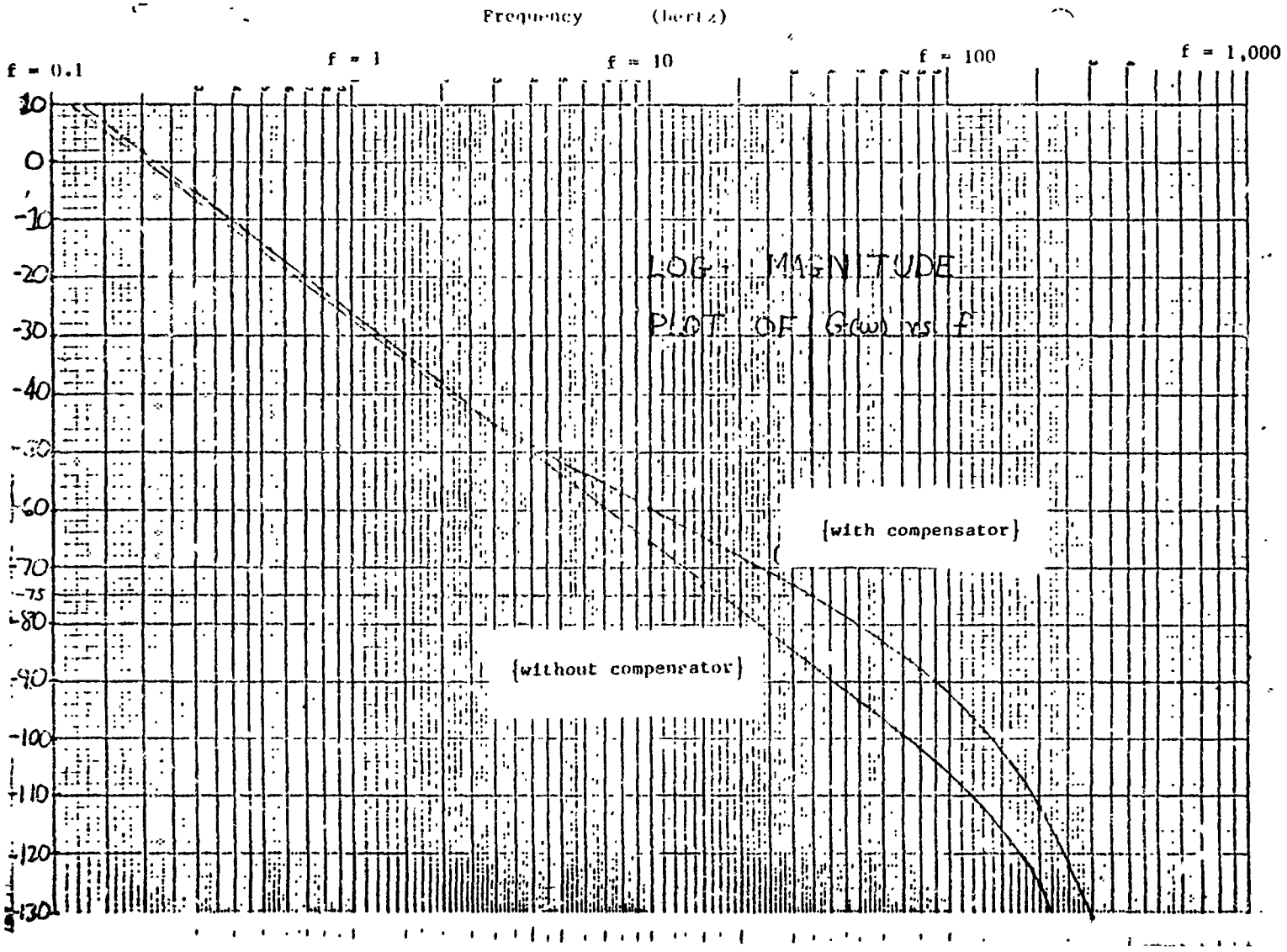

Figure 10a. Frequency Response (Log Magnitude) With and Without the Compensator

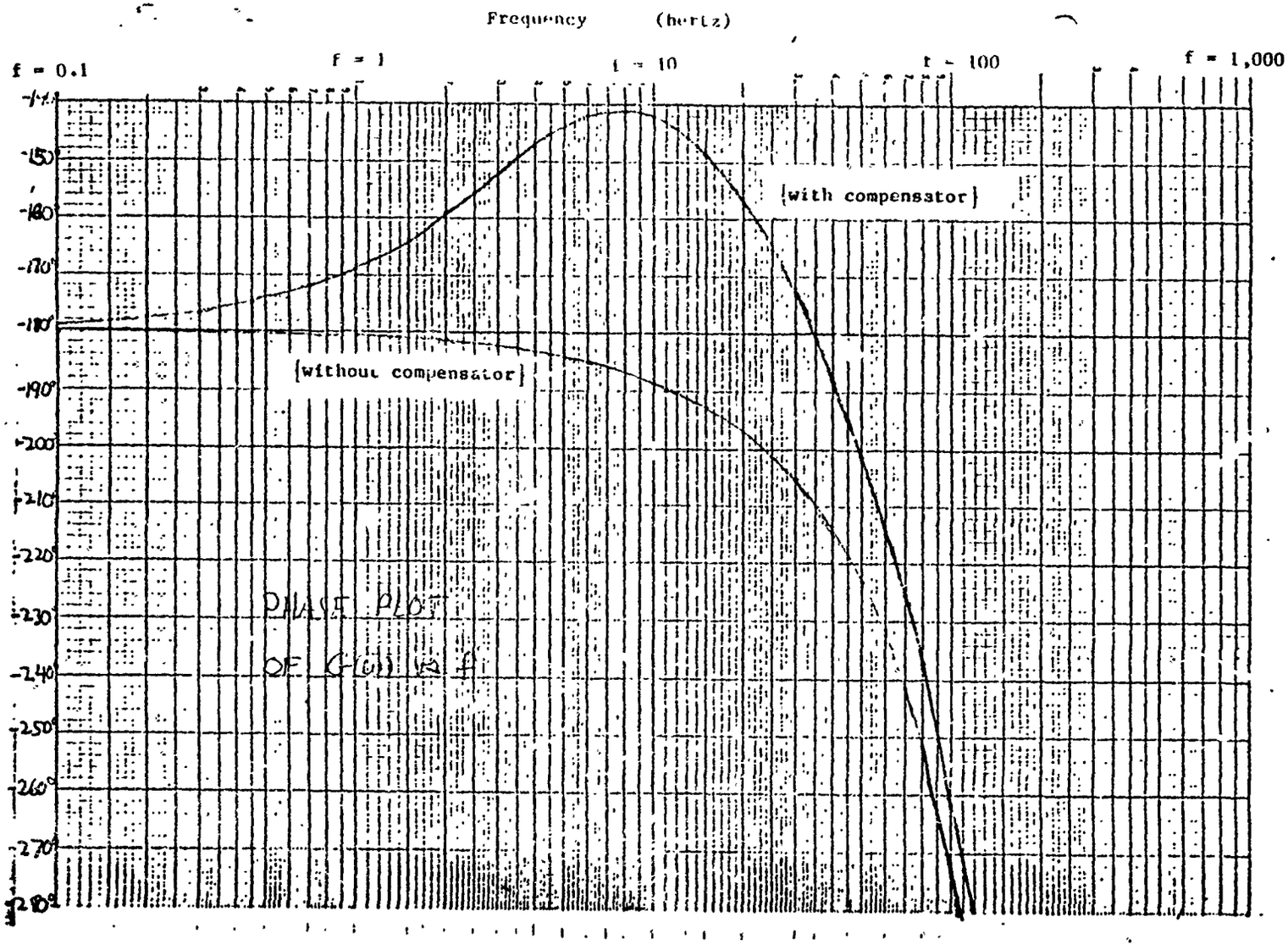

Figure 10b. Frequency Response (Phase) With and Without the Compensator

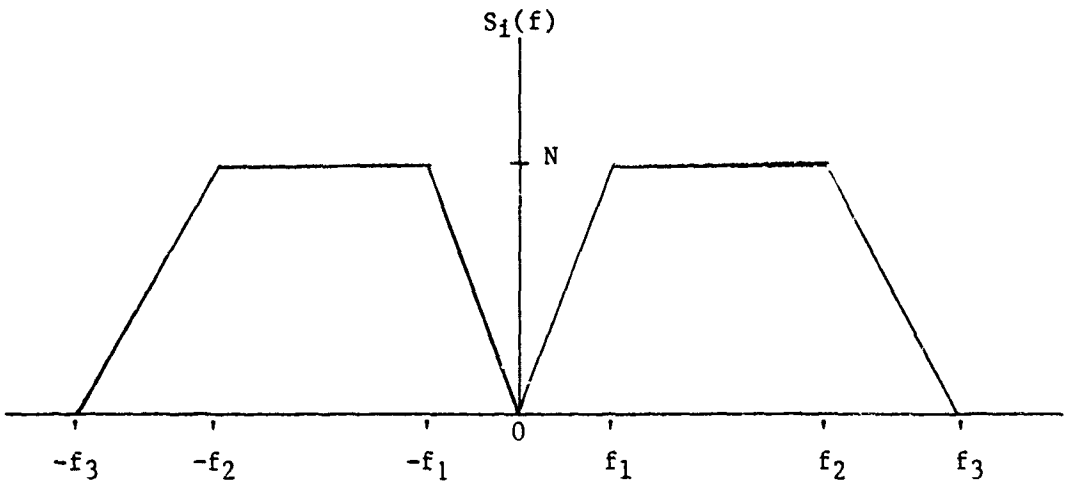

Figure 11. Spectral Density of the Input Noise to the Demodulation Process

The autocorrelation of this spectrum is

$$R_i(\tau) = -\frac{2N}{(2\pi\tau)^2} \left\{ \frac{1 - \cos(\omega_1\tau)}{f_1} + \frac{\cos(\omega_3\tau) - \cos(\omega_2\tau)}{f_3 - f_2} \right\}.$$

Its variance is $R_i(0) = A[f_3 + f_2 - f_1]$ which is the same value obtained when the spectrum $S_i(f)$ is integrated over all f

$$\sigma_{n_i}^2 = R_i(0) = \int_{-\infty}^{\infty} S_i(f)\, df.$$

Now, the output noise process can be modeled by

$$n_o(t) = n_i(t) \sin(\omega_d t + \theta)$$

where n_i has $R_i(\tau)$, $S_i(f)$ general characteristics, in particular, that specified above. Since the input noise is purely random in nature, it is uncorrelated with the modulation term $\sin(\omega_d t)$ or when it begins. Therefore, we can assume that the modulation term has an arbitrary phase which is uniformly distributed between 0 and 2π. The output correlation function is

$$\begin{aligned} R_o(\tau) &= E[n_o(t)\, n_o(t+\tau)] \\ &= E[n_i(t) \sin(\omega_d t+\psi)\, n_i(t+\tau) \sin(\omega_d(t+\tau)+\psi)] \\ &= E[n_i(t)\, n_i(t+\tau)]\, E[\sin(\omega_d t+\psi) \sin(\omega_d(t+\tau)+\psi)] \\ &= R_i(\tau)\, E[\cos(\omega_d\tau) - \cos(\omega_d(2t+\tau)+2\psi)]/2 \\ R_o(\tau) &= R_i(\tau) \cos(\omega_d\tau)/2. \end{aligned}$$

The spectral density of the output $S_o(f)$ is the Fourier Transform of $R_o(\tau)$.

$$S_o(f) = 1/2 \int_{-\infty}^{\infty} R_i(\tau) \cos(\omega_d \tau)\, e^{-j\omega\tau}\, d\tau$$

$$= 1/4 \int_{-\infty}^{\infty} R_i(\tau) \left[e^{-j(\omega-\omega_d)\tau} + e^{-j(\omega+\omega_d)\tau}\right] d\tau$$

$$S_o(f) = [S_i(f-f_d) + S_i(f+f_d)]/4.$$

Hence, the output spectral density, $S_o(f)$, is 1/4 the sum of two densities; one of which is the input density shifted left f_d, and one shifted to the right f_d

Depending on the value of f_d relative to f_1, f_2 and f_3; the shape of the output spectrum will have different characteristics. For example, Figure 12a shows the output spectrum, $S_o(f)$ for $\frac{f_1+f_2}{2} < f_d < f_2$

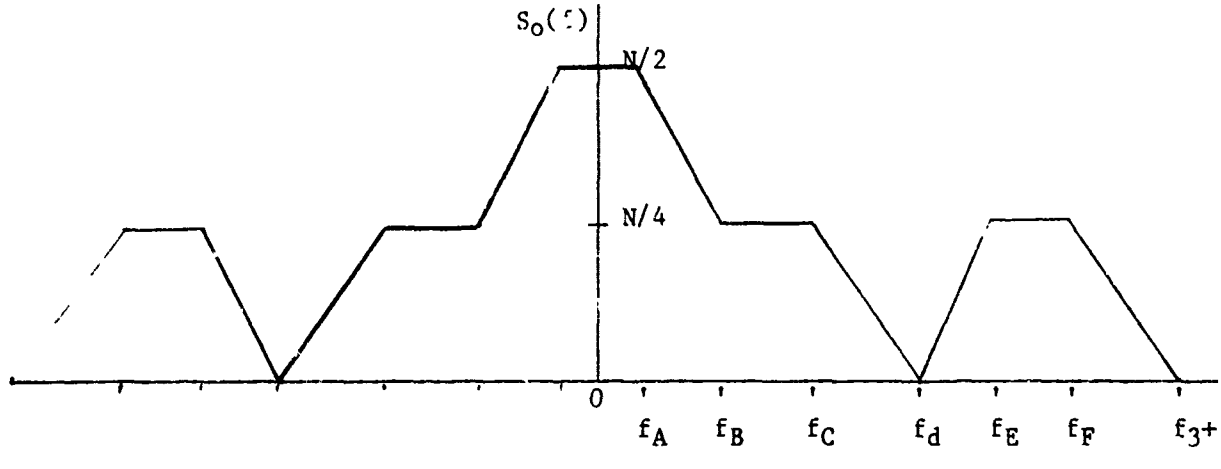

Figure 12a. Spectral Density of the Noise After Multiplication With the Dithered Signal - Large f_d

$f_A = f_2 - f_d$ $\qquad$ $f_E = f_1 + f_d$

$f_B = f_3 - f_d$ $\qquad$ $f_F = f_2 + f_d$

$f_C = f_d - f_1$

$$S_o(f) = 1/2 \int_{-\infty}^{\infty} R_i(\tau) \cos(\omega_d \tau)\, e^{-j\omega\tau}\, d\tau$$

$$= 1/4 \int_{-\infty}^{\infty} R_i(\tau) \left[e^{-j(\omega-\omega_d)\tau} + e^{-j(\omega+\omega_d)\tau}\right] d\tau$$

$$S_o(f) = [S_i(f-f_d) + S_i(f+f_d)]/4.$$

Hence, the output spectral density, $S_o(f)$, is 1/4 the sum of two densities; one of which is the input density shifted left f_d, and one shifted to the right f_d

Depending on the value of f_d relative to f_1, f_2 and f_3; the shape of the output spectrum will have different characteristics. For example, Figure 12a shows the output spectrum, $S_o(f)$ for $\frac{f_1+f_2}{2} < f_d < f_2$

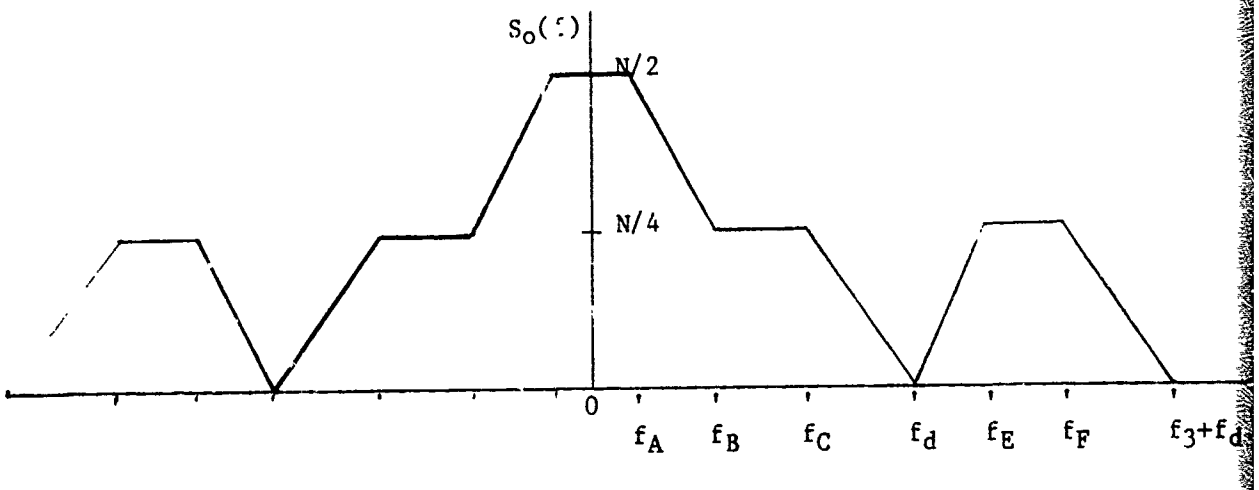

Figure 12a. Spectral Density of the Noise After Multiplication With the Dithered Signal - Large f_d

$f_A = f_2 - f_d$ $\qquad$ $f_E = f_1 + f_d$

$f_B = f_3 - f_d$ $\qquad$ $f_F = f_2 + f_d$

$f_C = f_d - f_1$

The variance of the output is the area under $S_o(f)$ which is

$$\sigma^2_{out} = 2\{ N[f_2 - f_d]/2 - Nf_1/4 + N[f_3 + f_d - (f_2 - f_d)]/4\}$$

$$= N[f_2 - f_d - f_1/2 + (f_3 - f_2 + 2f_d)/2]$$

$$= N[f_3 + f_2 - f_1]/2$$

$$\sigma^2_{out} = \sigma^2_{in}/2.$$

The output variance is 1/2 the input variance, but its spectrum has shifted with a flat spectrum about f=0 whereas the input has a "V" about f=0.

Figure 12b. shows the output spectrum, $S_o(f)$, for $f_1 < f_d < \frac{f_1+f_2}{2}$

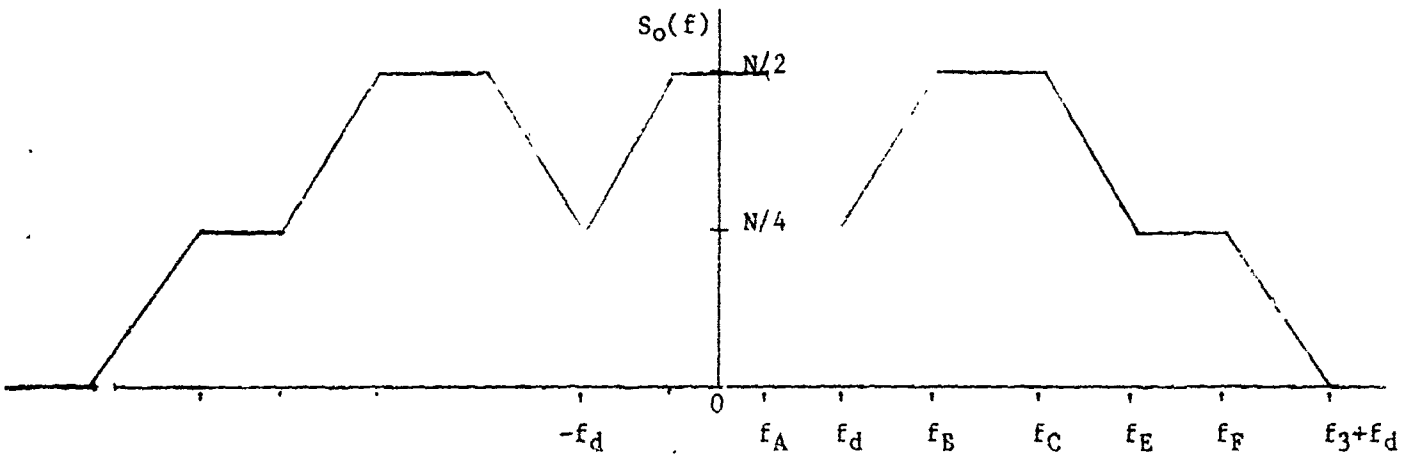

Figure 12b. Spectral Density of the Output Noise After Multiplication With the Dithered Signal - Small f_d

$f_A = f_d - f_1$ $\qquad$ $f_E = f_3 - f_d$

$f_B = f_1 + f_d$ $\qquad$ $f_F = f_2 + f_d$

$f_C = f_2 - f_d$

The variance of the output is, again, the area under $S_o(f)$:

$$\sigma^2_{out} = 2\,\frac{N}{4}\,\{(f_2+f_d) + (f_2-f_1-2f_d) + (f_d-f_1) + (f_3-f_2) + f_1\}$$

$$= \frac{N}{2}[f_3+f_2-f_1]$$

$$\sigma_{out}^2 = \sigma_{in}^2/2$$

Again, the spectrum is flat about f=0 whereas the input has a "V" about f=0.

This output spectrum is then passed through a low pass filter. The noise spectrum of the feedback output is

$$S_{fo}(f) = |H(j\omega)|^2 S_o(f)$$

where $H(j\omega)$ is the combined transfer function of the filter/control/mirror feedback subsystem. There are two types of feedback systems, Type I and Type II systems to be considered. With a Type II system,

$$H_{II}(s) = \frac{KH_o(s)}{s^2}$$

where $H_o(s)$ is the Type 0 portion of the subsystems. Assuming that K = 1 and since the effects of $H_o(s)$ is negligible at low frequencies, then the spectrum of the output filter/control is

$$S_{fc}(f) = \frac{S_o(f)}{(2\pi)^4 f^4} .$$

Approximating $S_o(f)$ to be uniform between $\pm f_2$, then

$$S_{fo}(f) = \frac{N}{2(2\pi)^4 f^4} \quad ; -f_2 \leq f \leq f_2 .$$

The autocorrelation function of the feedback output is the inverse Fourier transform which is

$$R_{fo}(\tau) = 1/2\pi \int_{-\infty}^{\infty} S_{fo}(f)\, e^{j\omega\tau}\, d\omega$$

$$= 1/2\pi \int_{-\omega_2}^{\omega_2} N/2\omega^4\, e^{j\omega\tau}\, d\omega .$$

The noise variance at the feedback output is $R_{fo}(0)$which is the area under the spectrum

$$\sigma_{fo}^2 = 2 \int_0^{f_2} \frac{N}{2(2\pi)^4} \frac{df}{f^4}$$

$$= \frac{-N}{3(2\pi)^4 f^3} \Bigg|_0^{f_2}$$

and a limiting process must be applied

$$\sigma_{fo}^2 = \frac{N}{3(2\pi)^4} \left[\lim_{a\to o} 1/a^3 - 1/f_2^3\right]$$

the above becomes unbounded as $a \to 0$. This implies that the realization of the noise may be any value.
Consider the case where we have a type I system

$$H_I(s) = KH_o(s)/s.$$

As before, assume $K = 1$ and since the effects of $H_o(s)$ is negligible at low frequencies, then the output spectrum is

$$S_{fo}(f) = \frac{S_o(f)}{(2\pi)^2 f^2} .$$

Again, as before, if $S_o(f)$ is uniform in the region $-f_2 \leq f \leq f_2$, then

$$S_{fo}(f) = \frac{N}{2(2\pi)^2 f^2} \quad ; -f_1 \leq f \leq f_2.$$

The noise variance is the area under this spectrum

$$\sigma_{fo}^2 = 2 \int_o^{f_2} \frac{N}{2(2\pi)^2} \frac{df}{f^2}$$

$$= \frac{-N}{(2\pi)^2 f} \Bigg|_0^{f_2}$$

Again, as before, the above is evaluated using a limiting process;

$$\sigma_{fo}^2 = \frac{N}{(2\pi)^2} \{\lim_{a\to o} 1/a - 1/f_2\}$$

which becomes unbounded and the same results hold.

C. Signal and Noise Transfer for the Gaussian Glint Process (about $y = 0$, σ_g).

The signal and noise transfer characteristics of the gaussian glint process can be seen by the following approximation process. Consider a Taylor series expansion of the gaussian glint process about some point $y_o = \theta$ due to a small signal and noise

$$y(t) = \theta + A \sin(\omega_d t)$$

$$f(y) = \exp(-y^2/2\sigma_g^2) = \sum_{i=0}^{\infty} \frac{\partial^i f}{\partial y^i} \Bigg|_{y=\theta} \frac{(y - \theta)^i}{i!} .$$

The various (first 4) derivatives of the function f(y) are

$$f(y) = \exp(-y^2/2\sigma_g^2)$$

$$f'(y) = (-y/\sigma_g^2)\exp(-y^2/2\sigma_g^2)$$

$$f''(y) = (y^2 - \sigma_g^2)\exp(-y^2/2\sigma_g^2)/\sigma_g^4$$

$$f'''(y) = (3y\sigma_g^2 - y^3)\exp(-y^2/2\sigma_g^2)/\sigma_g^6$$

$$f''''(y) = (y^4 - 6y^2\sigma_g^2 + 3\sigma_g^4)\exp(-y^2/2\sigma_g^2)/\sigma_g^8$$

There are two operating points of special interest

zero slope $f' = 0 \Longrightarrow y = 0$

maximum slope $f'' = 0 \Longrightarrow y = \pm\sigma_g$

Evaluation of the various derivatives under zero and maximum slope

$y = 0$; $f(y) = e^0 = 1$

$$f'(y) = 0$$

$$f''(y) = -1/\sigma_g^2$$

$$f'''(y) = 0$$

$$f''''(y) = 3/\sigma_g^4$$

$y = \sigma_g$; $f(y) = 1/\sqrt{e}$

$$f'(y) = -1/\sigma_g\sqrt{e}$$

$$f''(y) = 0$$

$$f'''(y) = 2/\sigma_g^3\sqrt{e}$$

$$f''''(y) = -2/\sigma_g^4\sqrt{e}$$

In Tabular form

	$y = 0$	$y = \sigma_g$
$f(y)$	1	$1/\sqrt{e}$
$f'(y)$	0	$-1/\sigma_g\sqrt{e}$
$f''(y)$	$-1/\sigma_g^2$	0
$f'''(y)$	0	$2/\sigma_g^3\sqrt{e}$
$f''''(y)$	$3/\sigma_g^4$	$-2/\sigma_g^4\sqrt{e}$

Maximum Slope:

Consider the maximum slope bias point. Using the first 4 terms of the series expansion about $y_o = \sigma_g$ with $y = \sigma_g + A \sin(\omega_d t) + n_i(t)$ where $n_i(t)$ is the input noise, the output is

$$z(t) = 1/\sqrt{e} \{1 - (A \sin(\omega t) + n_i(t))/\sigma_g + 0/2! + 2(A \sin(\omega t) + n_i(t))^3/\sigma_g^3\ 3! + \ldots\ \}$$

The most significant terms of the expansion are:

signal $\quad \{1 - A \sin(\omega t)/\sigma_g\}/\sqrt{e}$

noise $\quad n_i(t)/\sigma_g\sqrt{e}$

Hence, both the signal and noise process are preserved with a change in amplitude. At the maximum slope, the expected signal and noise terms are easy to understand and observe using the above simple example as illustrated by the frequency spectrum of Figures 13a and 13b.

Minimum Slope:

Using the first 4 terms of the series about $\theta = 0$ the output is

$$z(t) = 1 + 0/1!\ - (A \sin(\omega t) + n_i)^2/\sigma_g^2\ 2! + 0/3! + 3(A \sin(\omega t) + n_i)^4/\sigma_g^4\ 4! + \ldots$$

$$= 1 - [A^2 \sin^2(\omega t) + 2A \sin(\omega t)\ n_i(t) + n_i^2(t)]/2\sigma_g^2 + [A^4 \sin^4(\omega \tau) + \ldots + n_i^4(t)]/8\sigma_g^4 + \ldots$$

The most significant terms of the output are:

signal $\quad 1 - A^2 \sin^2(\omega t)\ /2\sigma_g^2$

noise $\quad [2\ n_i(t)\ A \sin(\omega t) + n_i^2(t)]/2\sigma_g^2$

Hence, both the signal and noise process change at the zero glint bias point. Due to the extreme non-linearity at this point, both the output signal and noise change characteristics the modulation signal amplitude is now at twice the original frequency. The output noise has two components, one modulated by the dither frequency and one modulated by itself. These two modulated noise terms will give rise to spectrum components not present at the input as illustrated by Figure 13c.

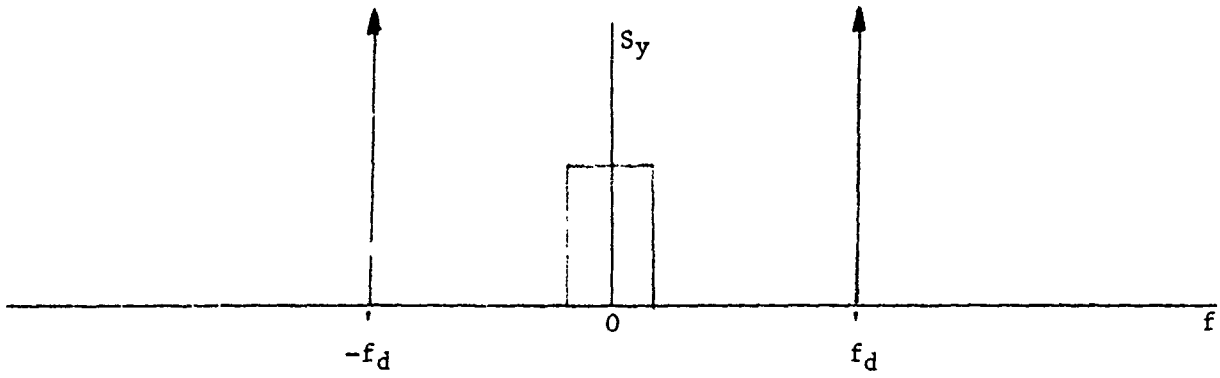

Figure 13a. Frequency Spectrum of a Signal and Noise at the Input of the Gaussian Glint

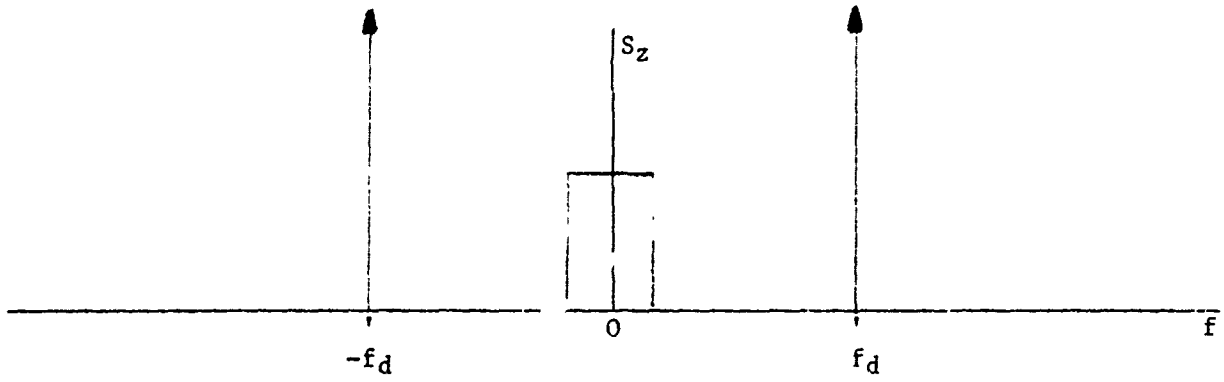

Figure 13b. Frequency Spectrum of the Output of the Gaussian Glint Process with the Operating Point $\theta_b = \sigma_g$

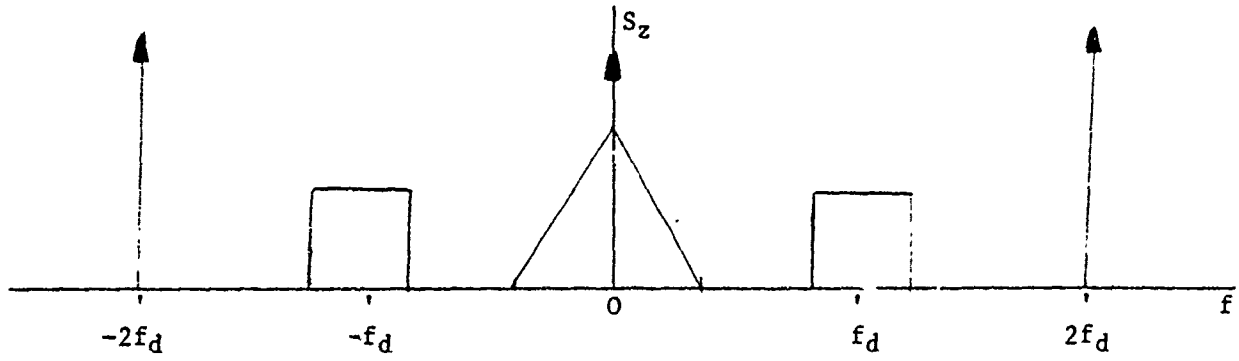

Figure 13c. Frequency Spectrum of the Output of the Gaussian Glint Process with the Operating Point $\theta_b = 0$

IV. Extended Kalman Filter for Laser Tracking

A. Extended Kalman Filter

A straight-forward application of an Extended Kalman Filter [3] for the bias angle estimation yields the following set of equations to be implemented.

$$\dot{\hat{\theta}}_b = K(t)[z(t) - g(\hat{y},t)]$$

$$y(t) = \theta_b + A \sin(\omega t)$$

$$g(\hat{y},t) = I_o \exp(-\hat{y}^2/2\sigma_g^2)$$

$$K(t) = -\frac{V_{\tilde{\theta}}}{\sigma_n^2}\frac{\hat{y}}{\sigma_g^2} g(\hat{y},t)$$

$$\dot{V}_{\tilde{\theta}} = -\frac{V_{\tilde{\theta}}^2}{\sigma_n^2}\frac{\hat{y}^2}{\sigma_g^4} g^2(\hat{y},t)$$

Note that:

$$\dot{V}_{\tilde{\theta}} = -K^2(t)\sigma_n^2$$

Figure 14. is a block diagram for the above filtering process.

B. Fourier Series Decomposition of the Extended Kalman Filter

The following will be a decomposition of this filter into the Fourier Series representation of the filtering process. As shown earlier, the Taylor Series expansion of the gaussian glint process about a point θ is

$$f(y) = \sum_{i=0}^{\infty} \frac{\partial^i f}{\partial y^i}\bigg|_{y=\theta} \frac{(y-\theta)^i}{i!}.$$

With the input

$$y = \theta + A \sin(\omega_d t),$$

then

$$f(y) = e^{-\theta^2/2\sigma_g^2}\left\{1 - \frac{\theta}{\sigma_g^2} A \sin(\omega_d t) + \frac{\theta^2 - \sigma_g^2}{\sigma_g^4\ 2!} A^2\sin^2(\omega_d t)\right.$$

$$\left. + \frac{3\theta\sigma_g^2 - \theta^3}{\sigma_g^6\ 3!} A^3\sin^3(\omega_d t) + \frac{\theta^4 - 6\theta^2\sigma_g^2 + 3\sigma_g^4}{\sigma_g^8\ 4!} A^4\sin^4(\omega_d t) + \ldots\right\}$$

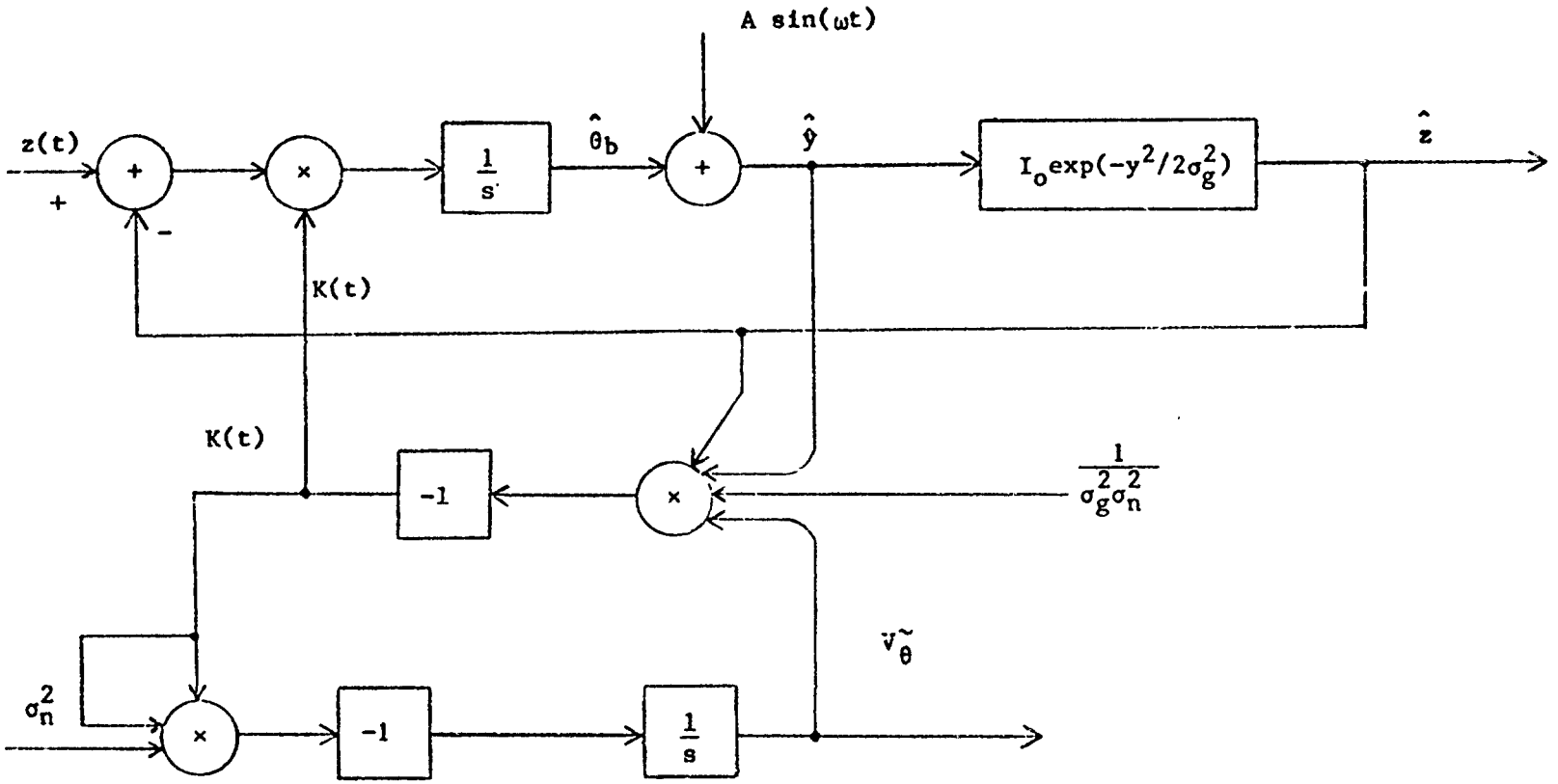

Figure 14. The Extended Kalman Filter for the Gaussian Glint Process

The Kalman filtering gain is

$$K(t) = \frac{-V_{\tilde{\theta}}\, y}{\sigma_n^2\, \sigma_g^2}\; g(y)$$

where $V_{\tilde{\theta}}$ is the error variance

$$g(y) = I_o f(y), \text{ and } y = \theta + A \sin(\omega_d t),$$

then

$$K(t) = \frac{-V_{\tilde{\theta}}}{\sigma_n^2\, \sigma_g^2}\; [\theta + A \sin(\omega_d t)]\; I_o\; e^{-\theta^2/2\sigma_g^2}\; [\cdot]\;.$$

Let

$$L(V_{\tilde{\theta}}, \theta) = \frac{-V_{\tilde{\theta}} I_o e^{-\theta^2/2\sigma_g^2}}{\sigma_n^2\, \sigma_g^2}\;, \text{ then}$$

$$K(t) = L\,[\theta + A \sin(\omega_d t)]\; \{1 - \frac{\theta}{\sigma_g^2} A \sin(\omega_d t) + \frac{\theta^2 - \sigma_g^2}{\sigma_g^4\, 2!} A^2 \sin^2(\omega_d t)$$

$$+ \frac{3\theta\sigma_g^2 - \theta^3}{\sigma_g^6\, 3!} A^3 \sin^3(\omega_d t) + \frac{\theta^4 - 6\theta^2\sigma_g^2 + 3\sigma_g^4}{\sigma_g^8\, 4!} A^4 \sin^4(\omega_d t) + \cdots\}$$

$$= L\,\{C_o + C_1 \sin(\omega_d t) + C_2 \sin^2(\omega_d t) + C_3 \sin^3(\omega_d t) + C_4 \sin^4(\omega_d t) + \cdots\}$$

where

$$C_o = \theta$$

$$C_1 = A\,[\frac{\sigma_g^2 - \theta^2}{\sigma_g^2}]$$

$$C_2 = \frac{A^2}{2!}\,[\frac{\theta^3 - \theta\sigma_g^2}{\sigma_g^4} - \frac{2!\,\theta}{\sigma_g^2}]$$

$$= \frac{A^2}{2!}\,[\frac{\theta^3 - 3\theta\sigma_g^2}{\sigma_g^4}]$$

$$C_3 = \frac{A^3}{3!}\,[\frac{3\theta^2\sigma_g^2 - \theta^4}{\sigma_g^6} + \frac{3!}{2!}\,(\frac{\theta^2 - \sigma_g^2}{\sigma_g^4})]$$

$$= \frac{A^3}{3!}\,[\frac{-\theta^4 + 6\theta^2\sigma_g^2 - 3\sigma_g^4}{\sigma_g^6}]$$

$$C_4 = \frac{A^4}{4!}\,[\frac{\theta^5 - 6\theta^3\sigma_g^2 + 3\theta\sigma_g^4}{\sigma_g^8} + \frac{4!}{3!}\,\frac{3\theta\sigma_g^2 - \theta^3}{\sigma_g^6}]$$

$$= \frac{A^4}{4!}\,[\frac{\theta^5 - 10\theta^3\sigma_g^2 + 15\theta\sigma_g^4}{\sigma_g^8}]$$

Using the various identities for $\sin^n(\alpha)$, i.e.

$$\sin^2(\alpha) = [1 - \cos(2\alpha)]/2$$

$$\sin^3(\alpha) = [3\sin(\alpha) - \sin(3\alpha)]/4$$

$$\sin^4(\alpha) = [\frac{3}{2} - 2\cos(2\alpha) + \frac{1}{2}\cos(4\alpha)]/4,$$

the first few terms of the Fourier series representation of the Kalman gain are

$$\dot{K}(t) = L\{a_o + \sum_{i=1}^{4} a_i \cos(i\omega_d t) + \sum_{i=1}^{4} b_i \sin(i\omega_d t)\}$$

$$a_o = C_o + \frac{1}{2} C_2 + \frac{3}{8} C_4 + \ldots$$

$$a_1 = 0$$

$$a_2 = -\frac{1}{2} C_2 - \frac{1}{2} C_4 + \ldots$$

$$a_3 = 0$$

$$a_4 = \frac{1}{8} C_4 + \ldots$$

$$b_1 = C_1 + \frac{3}{4} C_3 + \ldots$$

$$b_2 = 0$$

$$b_3 = -\frac{1}{4} C_3 + \ldots$$

$$b_4 = 0$$

The Kalman gain is used to develop the time derivative of the bias estimate by multiplying it with the measurement residual

$$\tilde{z}(t) = z(t) - \hat{z}(t)$$

and

$$\dot{\hat{\theta}}(t) = K(t)\ \tilde{z}(t)$$

Figure 15a illustrates the process of obtaining the estimate of the glint bias and Figure 15b is the process now being used to generate the estimate. It is obvious that the present process is a simplification of the optimum process in that:

1. only the information in the fundamental harmonic is used, and
2. the transfer gain is constant instead of the time varying optimum process.

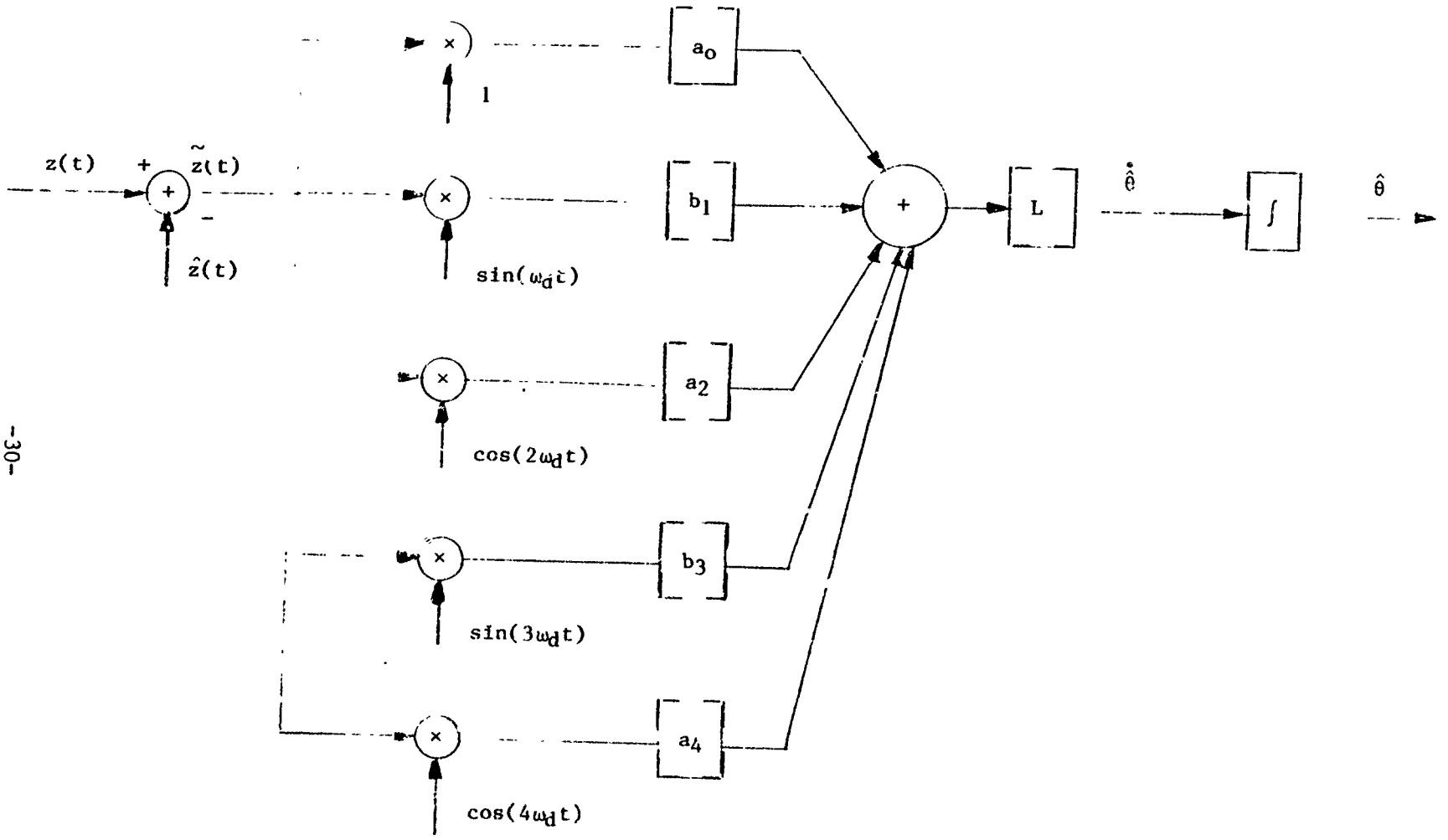

Figure 15a Kalman Process in Fourier Series Form to Estimate the Glint Bias

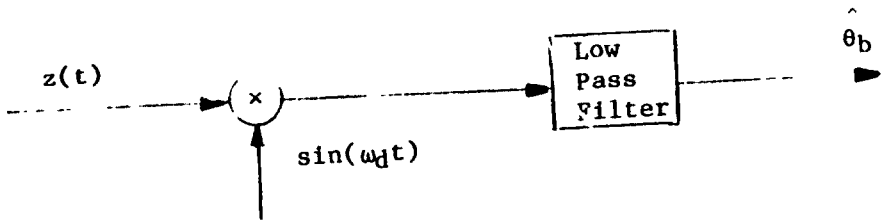

Figure 15b. Present Process to Estimate the Glint Bias

The second term of the Kalman Process illustrated on Figure 15a is similar to the present process of Figure 15b. In fact, the gain is an adaptive process of the glint bias

$$L\, b_1 = \frac{V_{\tilde{\theta}}\, I_o e^{-\theta^2/2\sigma_g^2}}{\sigma_n^2\, \sigma_g^2} (C_1 + \frac{3}{4} C_3)$$

Normalizing this bias term using $d = \theta/\sigma_g$

$$L\, b_1 = \frac{V_{\tilde{\theta}}\, I_o e^{-d^2/2}}{\sigma_n^2\, \sigma_g^2} [A(1 - d^2) + \frac{A^3}{8\sigma_g^2}(- d^4 + 6d^2 - 3)]$$

$$= \frac{V_{\tilde{\theta}}\, I_o}{\sigma_n^2\, \sigma_g^2} f(d)$$

where the following section describes the normalized gain function $f(d)/\sigma_g$.

C. Coefficient Evaluations for the Fourier Series $\{a_i, b_i\}$

The Fourier Series Coefficients $\{a_i, b_i\}$ for the Kalman gain can be evaluated using a glint bias to standard deviation normalized variable

$$d = \theta/\sigma_g.$$

This process will show the relative importance of each coefficient. The various coefficients are

$$a_o = d\sigma_g + \frac{A^2}{4\sigma_g}(d^3 - 3d) + \frac{A^4}{64\sigma_g^3}(d^5 - 10d^3 + 15d)$$

$$a_1 = 0$$

$$a_2 = - \frac{A^2}{4\sigma_g}(d^3 - 3d) - \frac{A^4}{48\sigma_g^3}(d^5 - 10d^3 + 15d)$$

$$a_3 = 0$$

$$a_4 = \frac{A^4}{192\sigma_g^3}(d^5 - 10d^3 + 15d)$$

$$b_1 = A(1 - d^2) + \frac{A^3}{8\sigma_g^2}(- d^4 + 6d^2 - 3)$$

$$b_2 = 0$$

$$b_3 = - \frac{A^3}{24\sigma_g^2}(- d^4 + 6d^2 - 3)$$

$$b_4 = 0$$

Figure 16a and 16b lists normalized values for these coefficients for various operating points $d = \{-1 \text{ to } 1\}$ which corresponds to a variety of glint bias θ_b points and for values of dither amplitude $A = 1/2\sigma_g$, and σ_g.

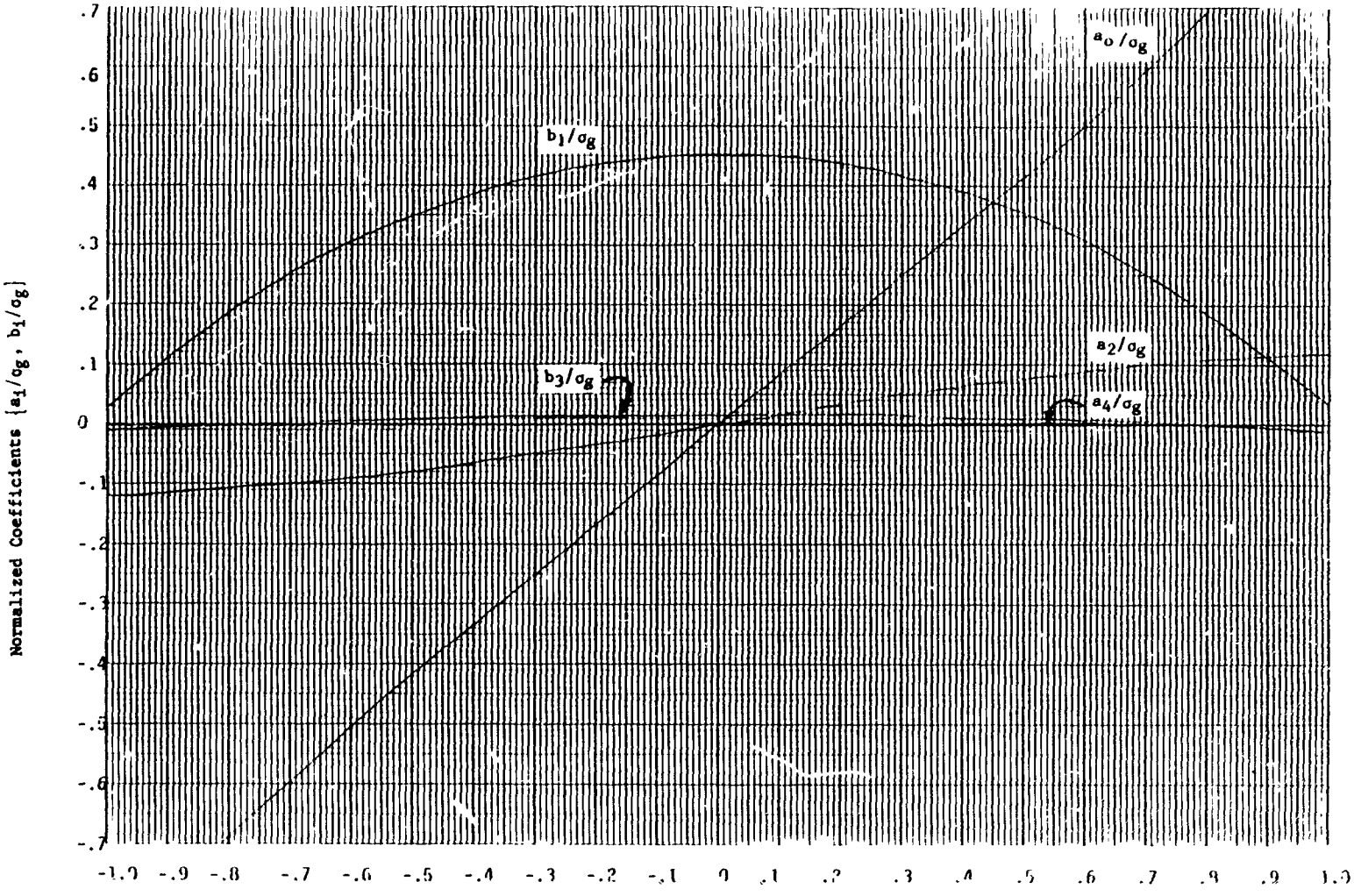

Figure 16a. Normalized Fourier Series Coefficients for $A = \frac{1}{2}\sigma_\xi$

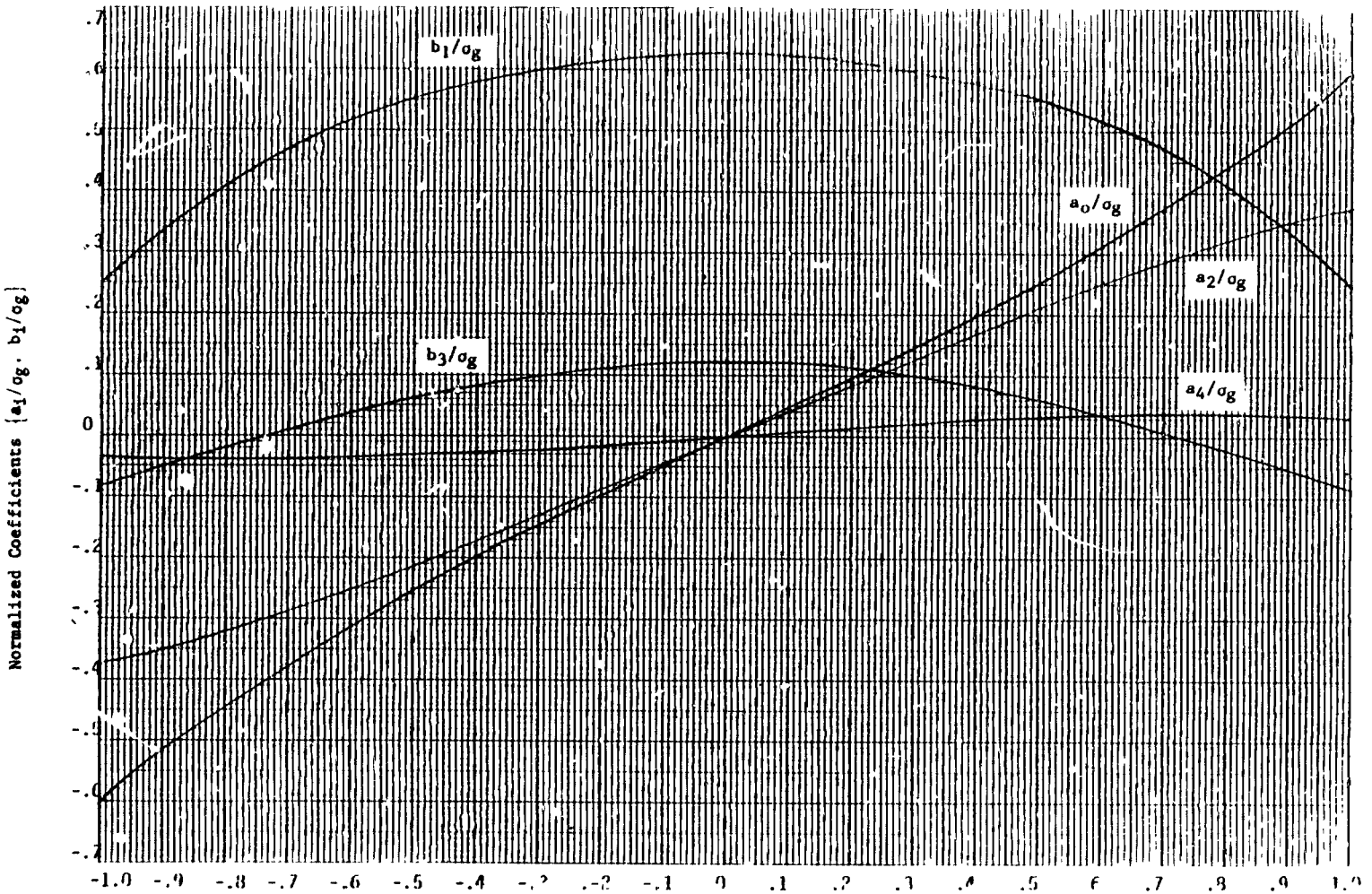

Figure 16b. Normalized Fourier Series Coefficients for $A = \sigma_g$

D. Optimal Estimation Error Variance (Bound)

The following will be a bounded closed form solution for the error variance. The error variance (using V for $V_{\tilde{\theta}}$) differential equation is

$$\dot{V} = - \frac{V^2 y^2 g^2(y,t)}{\sigma_n^2 \sigma_g^4}$$

where

$$y(t) = \theta + A \sin(\omega_d t), \text{ and } \quad g(y,t) = I_o \exp(-y^2/2\sigma_g^2),$$

then $$\dot{V} = -cV^2[\theta + A \sin(\omega_d t)]^2 \exp(-y^2/\sigma_g^2).$$

where $$c = \frac{I_o^2}{\sigma_n^2 \sigma_g^4} \quad \text{(constant)}.$$

Separating variables, the above can be expressed as

$$\frac{-dV}{V^2} = cy^2(t)\exp(-y^2/\sigma_g^2)dt.$$

Upon integrating,

$$\frac{1}{V(t)} - \frac{1}{V_o} = c\int_o^t y^2(\tau)\exp(-y^2(\tau)/\sigma_g^2)d\tau$$

where V_o is the initial condition on V. Since the exponential function can be bounded

$$\exp[-(|\theta| + |A|)^2/\sigma_g^2] \leq \exp(-y^2(t)/\sigma_g^2) \leq 1,$$

the above integral can be bounded by

$$\exp[\frac{-(|\theta| + |A|)}{\sigma_g^2}] \; F(t) \leq c \int_o^t y^2(\tau)\exp(-y^2/\sigma_g^2)d\tau \leq F(t),$$

where F(t) is a monotonically increasing function of time

$$F(t) = c \int_o^t [\theta + A \sin(\omega_d \tau)]^2 d\tau$$

$$= c \{(\theta^2 + A^2/2)t + 2A\theta(1-\cos(\omega_d t))/\omega_d - A^2 \sin(2\omega_d t)/4\omega_d\}.$$

The error variance can now be bounded

$$\frac{V_o}{1 + V_o F(t)} \leq V(t) \leq \frac{V_o}{1 + V_o F(t)\exp[-(|\theta|+|A|)^2/\sigma_g^2]}$$

E. Optimal Estimation Error Variance (Numerical Evaluation)

1. Numerical Solution

The differential equation of error variance for the Extended Kalman Filter [4] can be expressed as

$$\dot{V} = - c\, V^2\, y^2(t)\, \exp(-y^2(t)/\sigma_g^2)$$

where

$$c = \frac{\tau_o^2}{\sigma_n^2\, \sigma_g^4}$$

and

$$y(t) = \theta_b + A \sin(\omega_d t).$$

Separating variables and integrating yields

$$- \frac{dV}{V^2} = c\, y^2(t)\, \exp(-y^2(t)/\sigma_g^2)dt$$

$$\frac{1}{V(t)} = c \int_o^t y^2(\tau)\, \exp(-y^2(\tau)/\sigma_g^2)\, d\tau + \frac{1}{V_o}$$

and upon simplification, the error variance become

$$\boxed{V(t) = \frac{V_o}{1 + c\, V_o \int_o^t \{\cdot\}}}$$

where V_o is the initial error variance. Since the integrand is

$$\{\cdot\} = y^2(t)\, \exp(-y^2(t)/\sigma_g^2)$$

is a periodic function, then the integral can be evaluated at specific times which are integer multiples of T_d, the period of the dithered signal,

$$\int_o^{nT_d} \{\cdot\} = n \int_o^{T_d} \{\cdot\} .$$

The above one-period numerical integration process is easily obtained with the use of a sufficiently small integration step size ($\Delta\tau$).

2. Parametric Studies

Similar to the performance studies from the Information-Theoretic Bound (part II.B.), Figure 17 illustrates the numerical evaluation of the error variance, V(t), for signal-to-noise ratios of S/N = {1.0, 100, and 10,000} for a unity dithered amplitude and a null bias angle. The strong, direct influence of the S/N is apparent from the response illustrations of Figure 17 and the integral solution of V(t) where the multiplicative parameter "c" contains the signal-to-noise ratio.

Figure 18 illustrates the error variance response for various levels of dither amplitude with S/N = 100 and $\theta_b = 0$. The response, V(t), is shown to improve (decreases faster) as the dither amplitude increases, however, the rate of improvement decreases when at large values (i.e. from A = 5 to A = 10).

Varying the bias operating point, Figure 19 illustrates an improvement in the response V(t) as θ_b increases with a limiting effect at higher levels of bias (i.e. from $\theta_b = 5$ to $\theta_b = 10$).

3. Comparison of the Kalman Error Variance and the Information-Theoretic Bound

Two approaches have been used to evaluate the performance of the optimal angle estimation for the gaussian glint process. Although the Information-Theoretic and the Extended Kalman results are related to the same quantity, their interpertation and the assumptions made for their evaluations are different. However, they both give some measure as to the overall performance of the optimal angle estimation process as illustrated by Figure 20 which is nothing more than combining Figures 5 and 17. The results illustrate the lower bound attribute of the Information-Theoretic evaluation and the expected response when the Extended Kalman Filter is used.

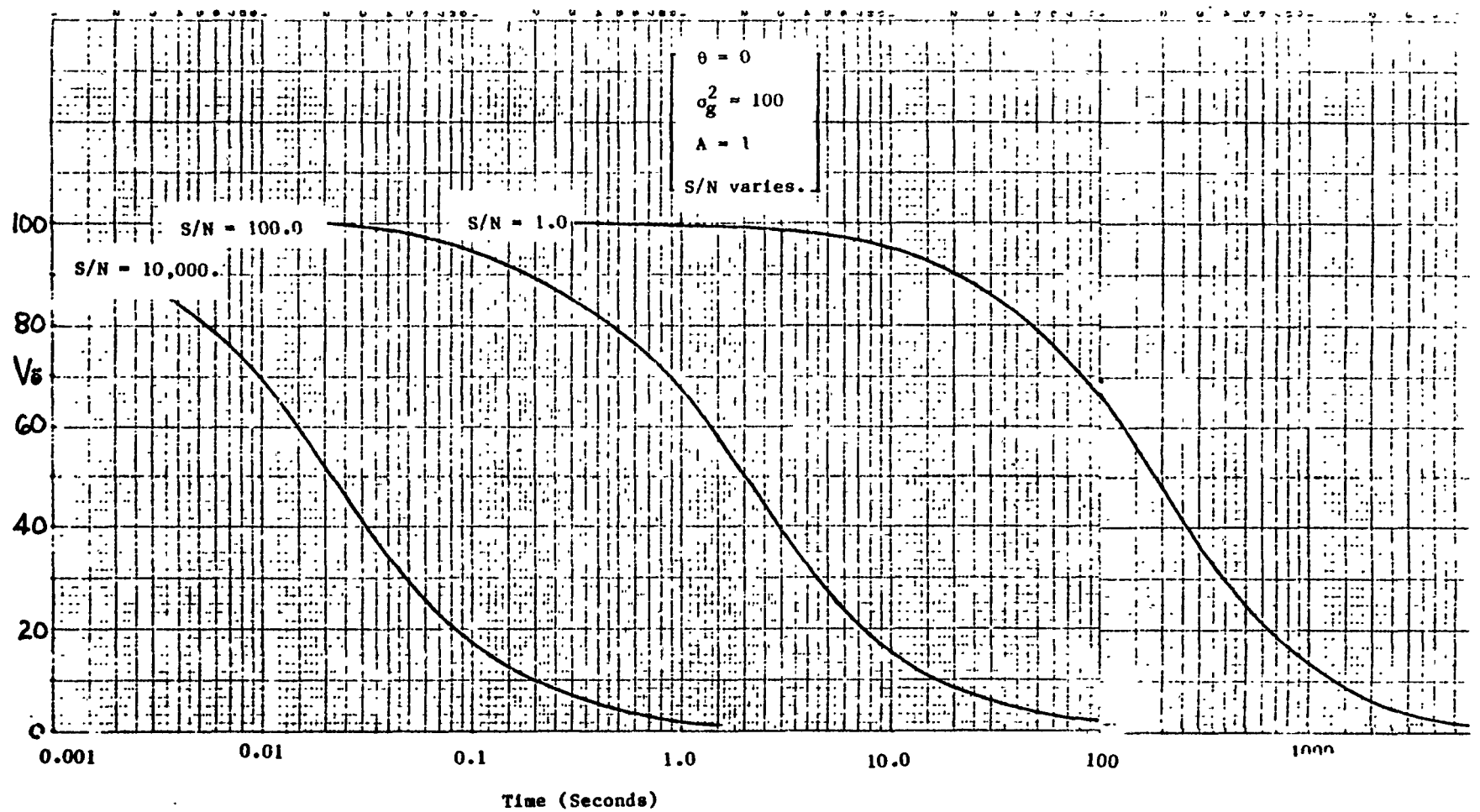

Figure 17 Extended Kalman Error Variance for Signal to Noise Variation

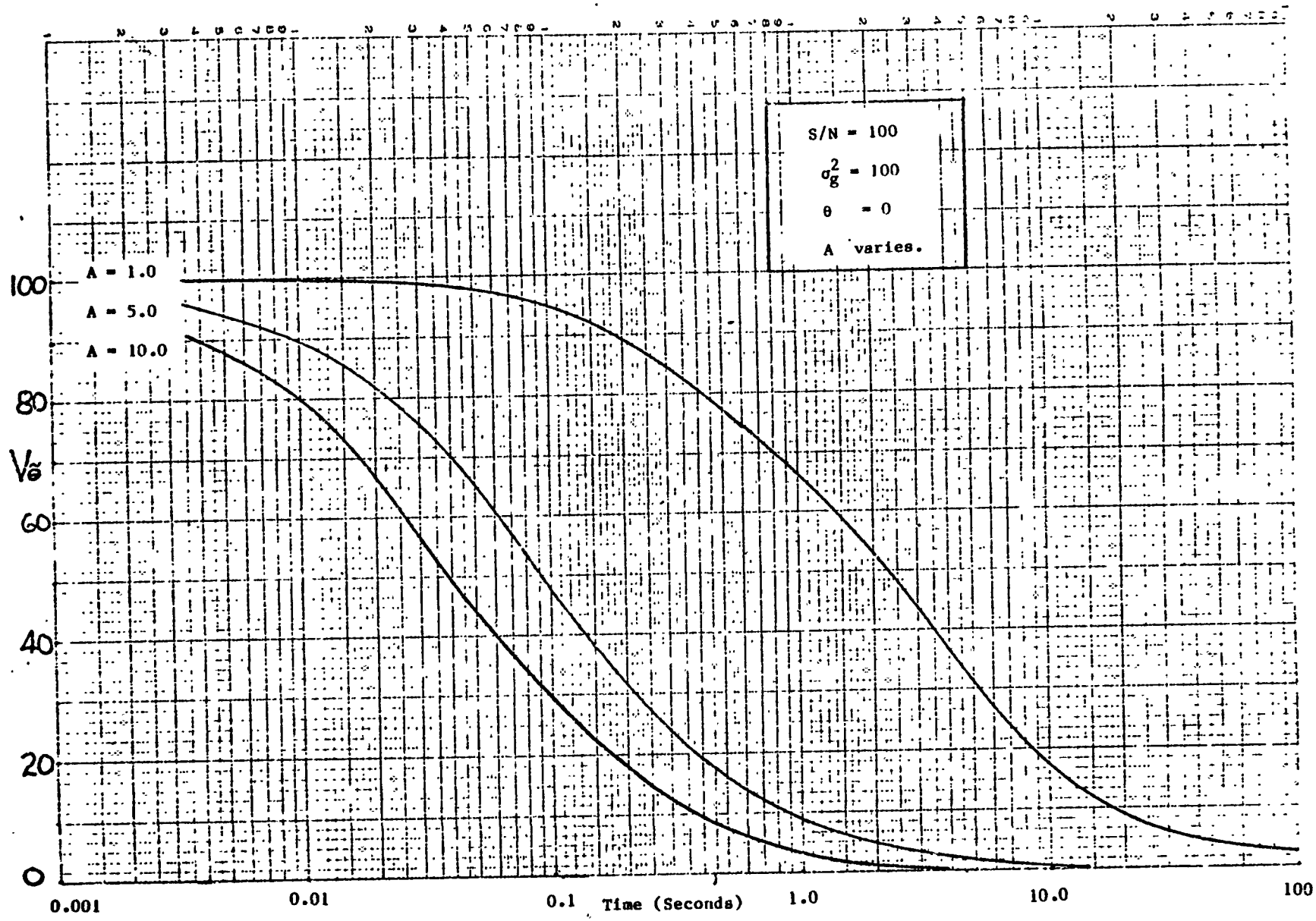

Figure 18. Kalman Error Variance for Dither Amplitude Variations

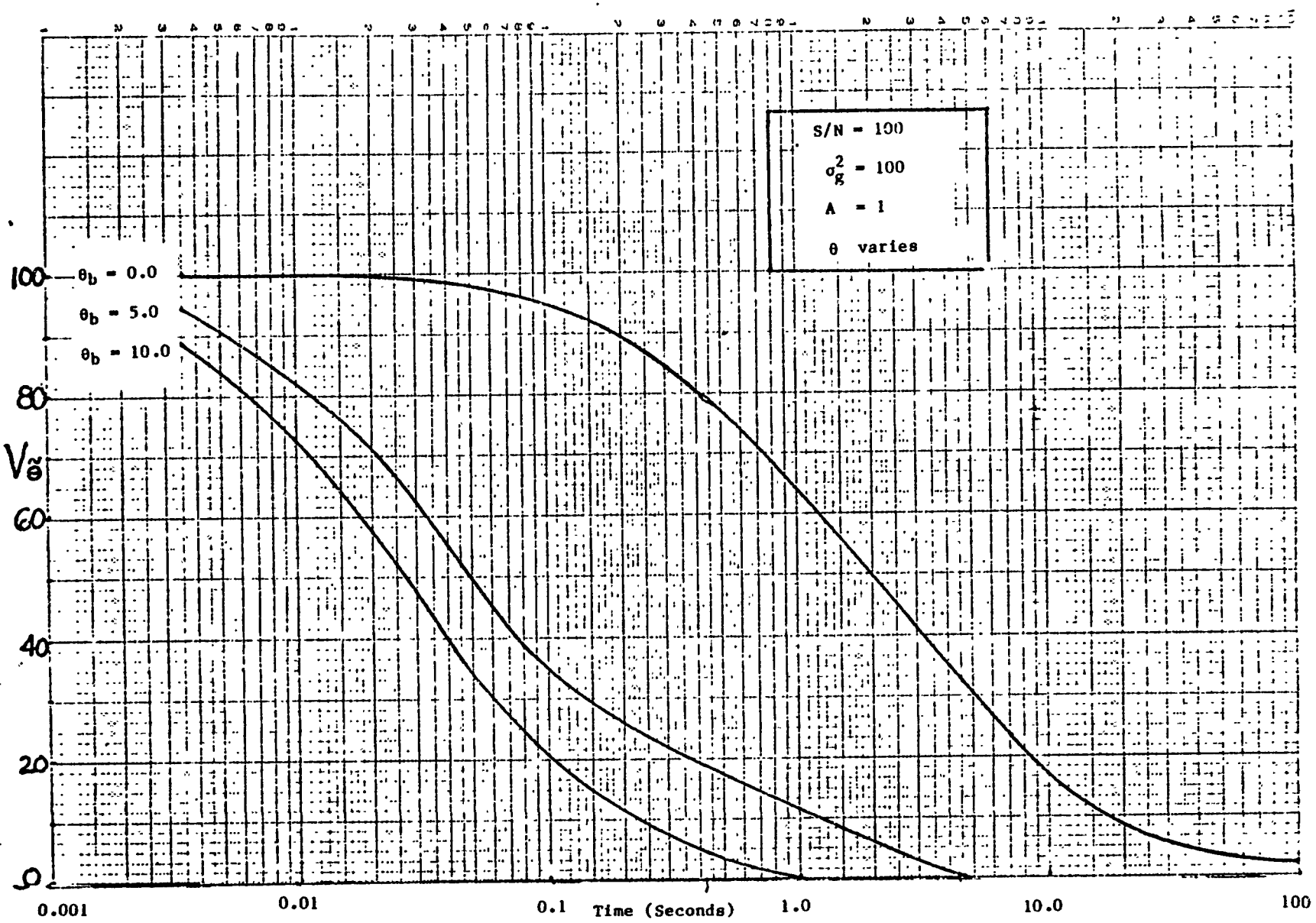

Figure 19. Kalman Error Variance for Bias Angle Variations

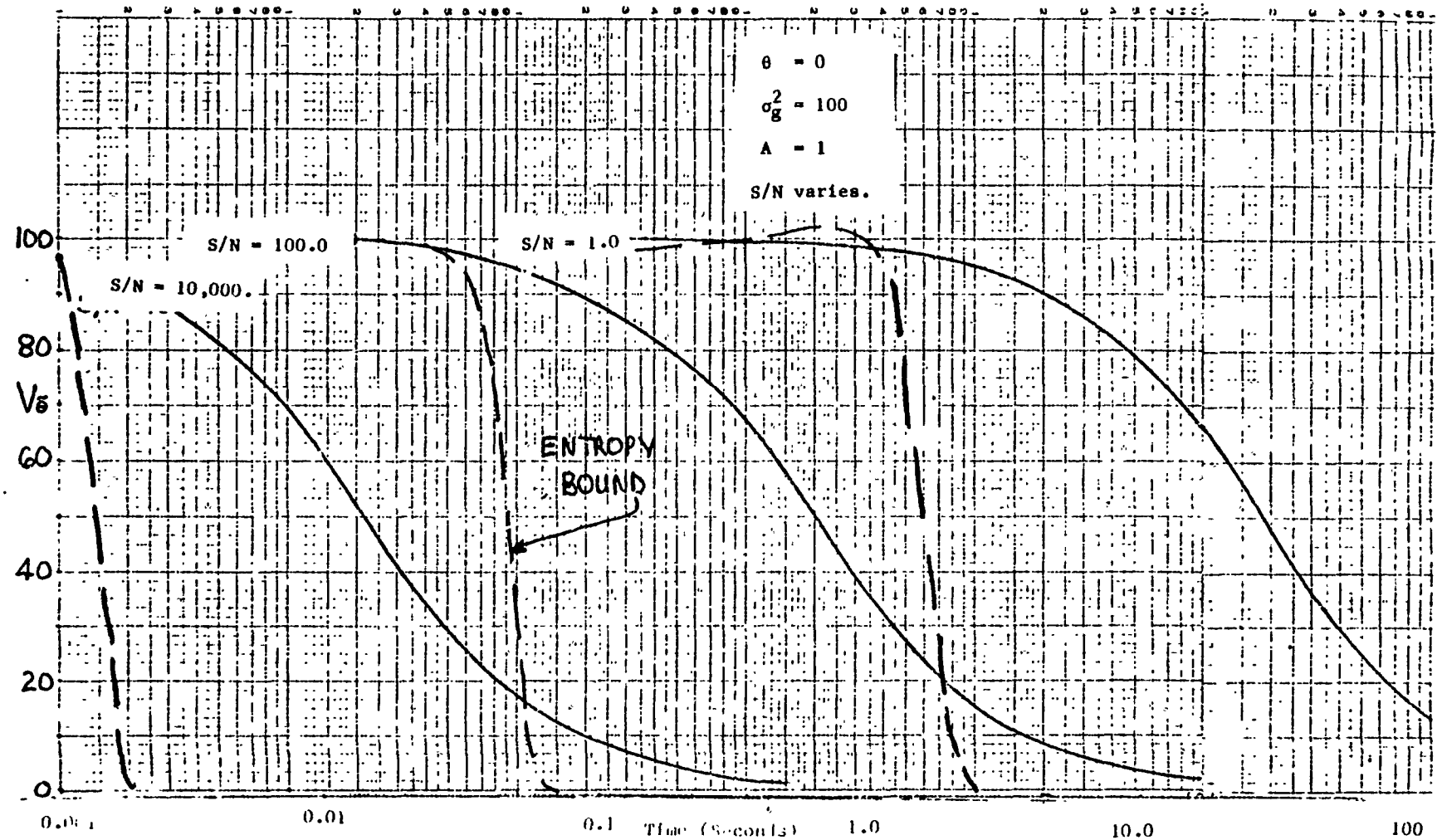

Figure 20. Comparison of the Information-Theoretic Bound and the Kalman Error Variance

V. Conclusion

A. Summary of Results

An Information-Theoretic Bound was found for the Laser Radar Tracking Problem. It was shown that the signal-to-noise ratio strongly affects the performance. There is also a slight variation in performance as a function of angle bias and signal amplitude but not a significant one.

An Informatic -Theoretical Analysis of the demodulation process showed that there was no loss of information due to the first step of the process, multiplication of the gaussian glint returned by the transmitted dithered signal. However, the suppression of the higher frequency components by the second step of the demodulation process, low pass filtering, destroys information contained the glint return.

The type II feedback transfer function is shown to be stabilized by the compensator where a deterministic positive gain margin is given. The first step of the demodulation process was shown to redistribute the noise spectrum contained in the output gaussian glint to significant levels at the low frequencies (D.C. region). Coupling this with the type II (or type I) feedback transfer function causes an unbounded stochastic variation.

The bias operating point has a strong effect on the spectral transfer function of the non-linear gaussian glint process. In particular, a small signal analysis showed that the zero bias operating point changes the deterministic and stochastic spectral response significantly. When the operating point is at the maximum slope, the output spectrum reflects the input spectrum.

The Extended Kalman Filter was applied to the open loop angle estimation problem involving a gaussian glint measurement with a dithered applied signal. Decomposing the filter formulation into a Fourier Series representation, it was shown:

i) the angle estimation process consists of a series of demodulation processes corresponding to various frequencies of the applied dither,

ii) the gains are chosen adaptively according to the bias angle, and

iii) the overall optimal error variance decreases monotonically as time increases.

The optimal adaptive filtering process presented is in the form similar to the present system and improvements can be made by using additional elements. Bounds on the optimal error variance were established in closed form and a numerical technique was also presented.

The error variance for the angle estimation is shown to be bounded and a numeric process is also presented. Evaluating the error variance for various parametric cases show a strong dependence on signal-to-noise. It is also shown that the dither amplitude and bias operating point has an effect on the estimation performance.

B. Extension

There are a number of natural extensions to the material presented in this paper:

i) Spectrum Analysis of the System

Items in this investigation would include both signal and noise transfers through the non-linear elements of the gaussian glint and the demodulation processes. The spectrum analysis of the closed loop controller and the Extended Kalman Filter will also be included.

ii) Parameter Variations of the Stochastic Control

There are various operating points and system parameters that yield optimum performance. A sensitivity study of these design parameters and operating points will be included.

iii) Adaptive Filter Implementation

There are two forms of the Extended Kalman Filter to be implemented. Each of these forms should be investigated as to their complexity of implementation. Also included in this investigation should be a sub-optimal filter which consists of the main element of the Optimal Filter. A performance analysis of this design will indicate the effects of the sub-optimal design.

iv) Optimal Controlling Process

The control process of the present system consists of a simple integrator on the bias error. An optimal design based on modern techniques which includes performance criterion of minimum settling time, control energy, jitter, etc. would be included.

Reference

1. Dillow, J., James, N. and Loos, C., "A Control Model for a Conical Scan Tracking System," AFWL-TR-76-131, Kirtland AFB.

2. Erteza, A., "Boresighting a Gaussian Beam on a Specular Target Point: A Method Using Conical Scan", Applied Optics, Vol. 15, March 1976.

3. Kalata, P.R., "An Information - Theoretic Approach to Target Estimation of a Conical Scan Controlled Laser Radar Tracking System," SCEEE/AFSOR Summer Faculty Research Program, 1981.

4. Haykin, S., Communication Systems, New York, Wiley, 1978.

5. Kalata, P.R., "An Information - Theoretic Approach to the Performance of Laser Radar Target Tracking Systems," AFSOR Proposal, 1981.

6. Merritt, P., Private Communications, Air Force Weapons Laboratory, Kirtland AFB.

7. Kalata, P., "An Information-Theoretic Approach to Estimation in Discrete Time Systems", Ph. D. Dissertation, Illinois Institute of Technology, May 1974.

8. Kalata, P. and Priemer, R., "On Minimal Error Entropy Stochastic Approximation", Int. J. Systems Science, Vol. 5, Sept. 1974.

9. Kalata, P. and Priemer, R., "On System Identification With and Without Certainty", J. Cybernetics, Vol. 8, 1978.

10. Kalata, P. and Priemer, R., "When Should Smoothing Cease?", Proc. IEEE, Vol. 62, Sept. 1974.

11. Kalata, P. and Priemer, R., "Linear Prediction, Filtering and Smoothing: An Information-Theoretic Approach", Information Sciences, Feb. 1979.

12. Zakai, M., and Ziv, J., "Lower and Upper Bounds on the Optimal Filtering Error of Certain Diffusion Processes," IEEE Trans. Information Theory, Vol. IT-18, May 1972.

13. Galdos, J., "A Lower Bound on Filtering Error with Application to Phase Demodulation," IEEE Trans. Information Theory, Vol. IT-25, July 1979.

14. Vidyasagar, M., Nonlinear Systems Analysis, Englewood Cliffs, New Jersey, Prentice-Hall, 1978.

15. Hughes Corporation, "Conical Scan Tracking," Discussions at AFWL, 1977.

Distribution

Dr. Bram, AFOSR, Bolling AFB, DC.
Capt. S. Fitzpatrick (3)
E.P. Brooks

Col. B. Francis, AFWL, Kirkland AFB, NM
Col. T. Johnson
Dr. A. Guenther
Col. D. Kyrazis
Col. J. Dillow
Col. J. Dettmer
Col. J. Janicke
Mr. R. Frosch
Maj. J. Terry
Ltc. B. O'Neil
Ltc. A. Halber
Maj. R. VanAllen (3)
Ltc. W. Hora
Col. K. Gilbert
Mr. D. Spreen
Col. D. Seegmiller
Ltc. D. Washburn
Mr. L. Sher
Ltc. T. Meyer
Maj. R. Brunson
Ltc. T. Meyer
Capt. Herrick
Capt. Holt
Dr. A. Erteza
Dr. J. Nichols
Capt. R. Rogers
Capt. W. Witt
Capt. D. Boesen
Maj. Allen

Dr. A. Stubberud, HQ USAF/CCN, Pentagon, Wash., D.C.
Dr. P. Merritt, Hughes Corp.
Ltc. C. O'Bryan
Dr. P. Kalata, Drexel University (10)